CHAPTER 1

INTRODUCTION

The genus *Heliotropium* consists of about 250 species that are distributed in tropical, subtropical and warm temperate regions of all continents. [1] The only one species found in Thailand is *Heliotropium indicum*. *H. indicum* commonly known in Thailand as "Yaa Nguang Chang" (หญ้างวงช้าง) and belongs to the family Boraginaceae [2], shown in the taxa classification of *H. indicum* as below;

1.1. Taxa and Classification of *Heliotropium indicum* Linn.[3]

Kingdom	: Plantae (Plant)
Subkingdom	: Tracheobionta (Vascular plants)
Superdivision	: Spermatophyta (Seed plant)
Division	: Magnoliophyta (Flowering plants)
Class	: Magnoliopsida (Dicotyledons)
Subclass	: Astridae
Order	: Lamiales
Family	: Boraginaceae (Borage family)
Genus	: *Heliotropium* L. (Heliotrope)
Species	: *Heliotropium indicum* Linn. (Indian heliotrope)

Plant Synonyms : *Heliotrpium anisophyllum*, *Triaridium indicum* (L.) Lehm., *Heliophytum indicum*, *Heliotropium parviflorum*.

Common names : Alacrancillo, Bhurundi, Clary, Clary wild, Cock's comb, Cola de Alacran, Cotorrera, Crete Coq, Crista de Gala, Damrey, Ditoyo, Dramoi, Erysipelas plant, Eye bright, Fedegoso, Hathisura, Hatisunda, Hatisura, Hattaguri, Herbe a malingre, Herbe a verrues, Herbe papillon, Hiebra del Alacran, Hoja de Alacran, Ihuin Rao, Jinkiukala, Kalil Tara Lal, Kantui Damrey, Merrino, Moco de Alote, Nangiku, Nasimko, Damrey, Plant Erysipelas, Promoi Damrey, Rumput Olet, Scarpontil, Scorpion weed, Ser-Bumi, Srikastini, Suryavarta, Tiliaguru, Tournesol Indien, Trompa Ng Elepante, Turnsole, Turnsoles, Ucullucui Sacha, Veveine Queue de Scorpion, Veven Lache Eskupyon, Voi Voi, Vrischikali, Yaa Nguang Chaang, Yerba de Borrajou, Yerba de Cotorra.

Figure 1 The inflorescence of *Heliotropium indicum* Linn.

H. indicum is a native of tropical America which is now widespread in all tropical regions of the world and generally grows in disturbed areas close to water

sources. This plant is an annual, erect, branched, hairy plant 15 to 50 centimeters in height. The leaves are opposite or alternate, ovate to ovate-oblong, 3 to 8 centimeters long, somewhat hairy, pointed at the tip, and widest near the rounded or heart-shaped base, and grow down along the petiole. The flowers are small, and borne on one side of curved, terminal, or leaf-opposed spikes which are 3 to 8 centimeters in length. The calyx is green. The corolla is pale lavender to nearly white, funnel-shaped, and about 5 millimeters long, with a slender and cylindric tube and the limb 3.5 mm in diameter. The fruit is 4 to 5 mm long, and is composed of 2, ovoid, beaked nutlets. [1]

Information from Natural Product Alert (NAPRALERT) data base developed by the University of Illinois at Chicago indicated that several type of compounds have been reported to be present in *H. indicum* and they can be classified in groups as follows;

1. Pyrrolizidine alkaloids
2. Triterpenoids
3. Steroids
4. Tannins
5. Flavonoids
6. Saponins
7. Miscellaneous compounds such as rapanone (**1**), spermine (**2**), spermidine (**3**), putrescine (**4**), hydrocyanic acid (**5**) and hexacosan-1-ol (**6**).

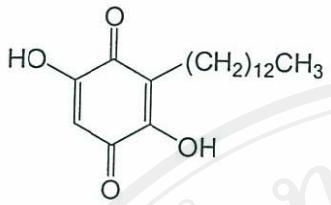

Rapanone (**1**)

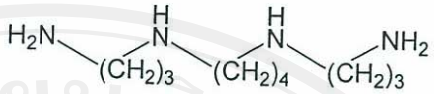

Spermine (**2**)

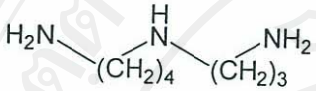

Spermidine (**3**)

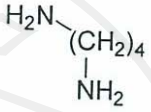

Putrescine (**4**)

Hydrocyanic acid (**5**)

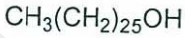

Hexacosane-1-ol (**6**)

The applications of *H. indicum* in traditional medicines throughout the world are summarized in Table 1. The significant biological activities of this plant are anti-inflammatory activity, diuretic activity, wound healing acceleration and hepatotoxic activity [4], antifertility effect [5], antitumor activity [6], antibacterial activity to *Pseudomonas aeruginosa*, *Stephylococcus aureus*, *Salmonella typhi* and *Escherichia coli* [7], antifungal activity to *Fusarium oxysporum* [8], uterine stimulant effect [9], smooth muscle relaxant activity [10], antispasmodic activity and hypotensive activity [11].

Table 1 Selected Ethonomedicinal applications of *H. indicum* in some countries.

Countries	Ethnomedicinal Applications	References
China	Herpes	[12]
Gambia	Venereal diseases	[4]
Guatemala	Relieving of fever	[13]
India	Emmenagogue (small doses), abortificient (large doses) and rheumatism	[4, 14 and 15]
Jamaica	Diuretic	[16]
Mexico	Treating of skin infections	[17]
Nicaragua	Coughs, insect bites and stings, diarrhea, relieving of fevers and treating of skin rashes	[18 and 19]
Peru	Abortifacient, anodyne, coughs, insect stings, rheumatism, diuretic, nephralgia, boils and treating of cancer	[20]
Philippines	Emmenagogue	[14]
Puerto Rico	Relieving of sore throats and ulcers	[4]
Taiwan	Hepatitis and liver disease	[21]
Thailand	Asthma and diuretic	[22 - 24]
Vietnam	Emmenagogue (small doses) and abortificient (large doses)	[25]

1.2 Chemistry of Compounds from *Heliotropium indicum* Linn.

Plants from the *Heliotropium* genus, e.g. *H. indicum* are known as a rich source of pyrrolizidine alkaloids; therefore phytochemical studies of this plant have been investigated and reported. Previous chemical analyses of the extracts from this plant have revealed several classes of compounds which can be summarized as follows.

1.2.1. Pyrrolizidines

Among the various compounds isolated from this plant, pyrrolizidines were found to be the most abundant class of chemical components. The seed of *H. indicum* was found to contain europine-*N*-oxide (**7**), heleurine-*N*-oxide (**8**), heliotridine-*N*-oxide (**9**), heliotrine-*N*-oxide (**10**) and lasiocarpine (**11**) as reported by Willaman and Schubert in 1961 [25]. In 1982, Pandey *et al.* reported the isolation of heliotrine (**12**) from the seed of this plant [11].

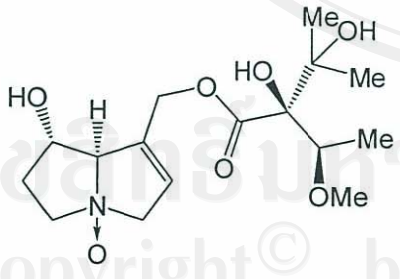

Europine-N-oxide (**7**)

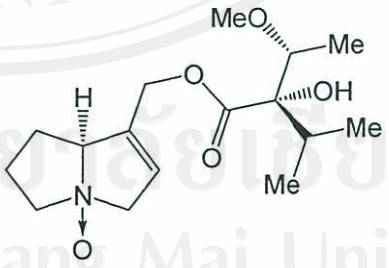

Heleurine-N-oxide (**8**)

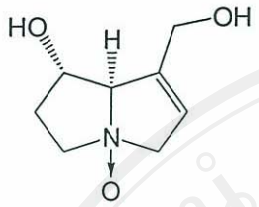

Heliotridine-N-oxide (**9**)

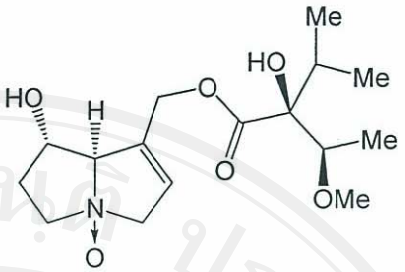

Heliotriine-N-oxide (**10**)

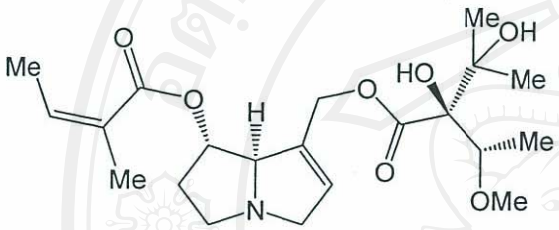

Lasiocarpine (**11**)

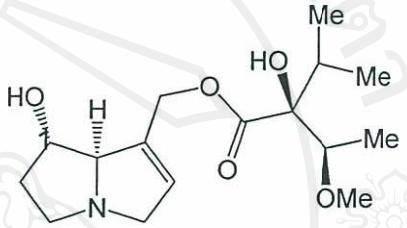

Heliotrine (**12**)

Pyrrolizidines from the methanol extract of the both aerial and entire part of *H. indicum*, revealed by Mattocks in 1961 [26] and 1967 [27] were indicine (**13**), indicine-*N*-oxide (**14**) [28 and 29] and acetyl indicine (**15**). Lasiocarpine (**11**), heliotrin (**12**), echinatine (**16**), heleurine (**17**), lasiocarpine-*N*-oxide (**18**), lindelofidine (**19**), retronecine (**20**), supinidine (**21**), supinine (**22**), and trachelanthamidine (**23**) were also found in the parts of this plant [25, 26, 30-34]. In 2005, Singh *et al.* [35] reported three pyrrolizidine alkaloids, acetyllasiocarpine (**24**), europine (**25**) and heliosupine (**26**) from the whole plant of *H. indicum*. This was the first report of these alkaloids in *H. indicum*.

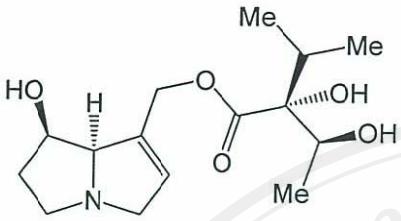

Indicine (**13**)

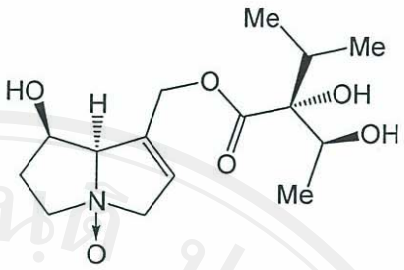

Indicine-N-oxide (**14**)

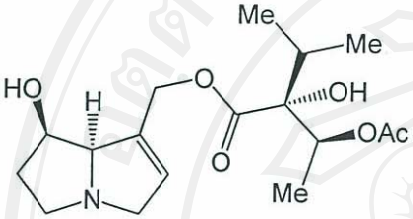

Acetyl indicine (**15**)

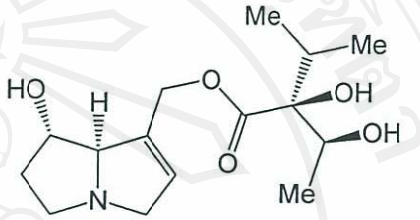

Echinatine (**16**)

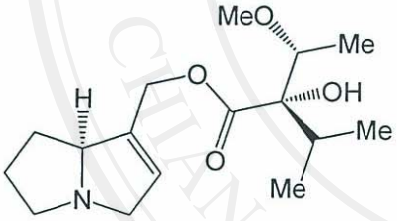

Heleurine (**17**)

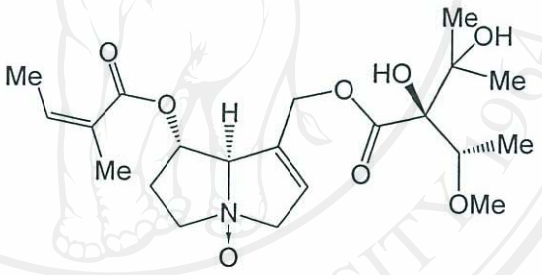

Lasiocarpine-N-oxide (**18**)

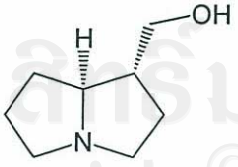

Tachelanthamidine (**23**)

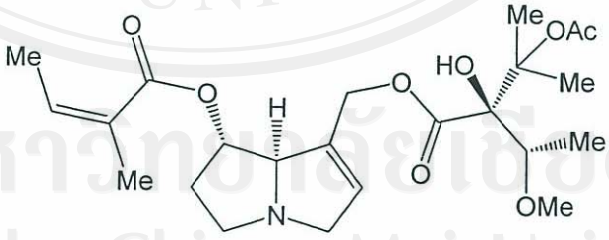

Acetyl lasiocarpine (**24**)

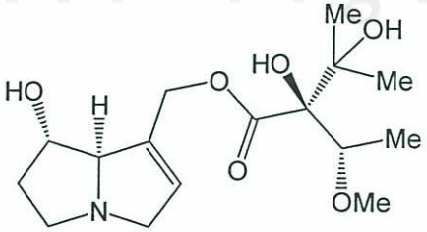

Europine (**25**)

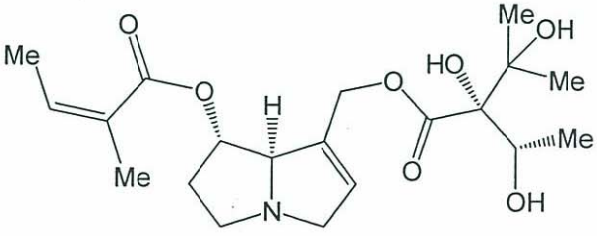

Heliosupine (**26**)

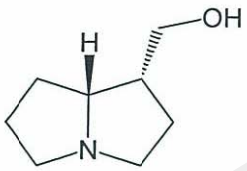

Lindelofidine (**19**)

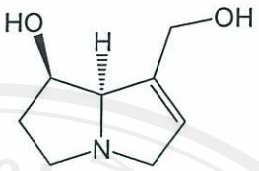

Retronecine (**20**)

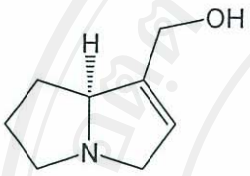

Supinidine (**21**)

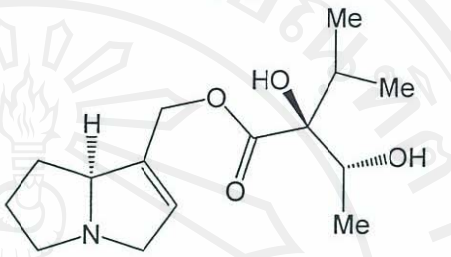

Supinine (**22**)

In 1984, Birecka reported the isolation of retronecine (**20**) from the leaves and inflorescences of *H. indicum* [34]. The roots of this plant were found to contain a new pyrrolizidine, helindicine (**27**) together with the known alkaloids lycopsamine (**28**) as reported by Souza *et al*. in 2005 [36].

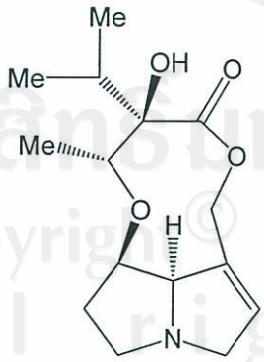

Helindicine (**27**)

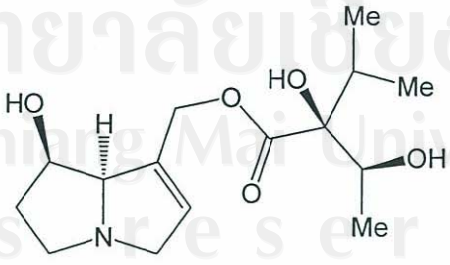

Lycopsamine (**28**)

Miscellaneous alkaloids, spermine (**2**), spermidine (**3**) and putrescine (**4**), from the leaves and the inflorescences of *H. indicum* were reported by Birecka in 1984 [34].

1.2.2 Steroids

In 1985, Andhiwal *et al.* [5] reported the isolation of campesterol (**29**) and stigmasterol (**30**), from the extract of the entire plant of *H. indicum*. Two years later, *β*-sitosterol (**31**) and its glucoside (**32**) were also found from this plant [31, 37]. Steroid found in the roots of *H. indicum* was estradiol (**33**) as reported by Manan and Ahmad in 1976 and 1978 [38, 39].

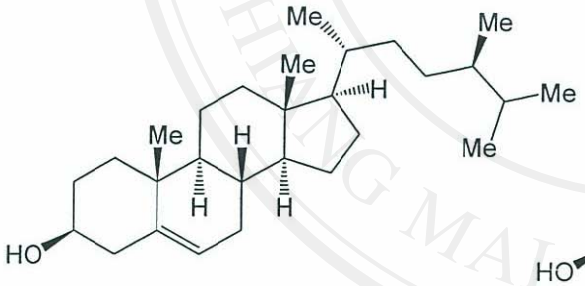

Campesterol (**29**)

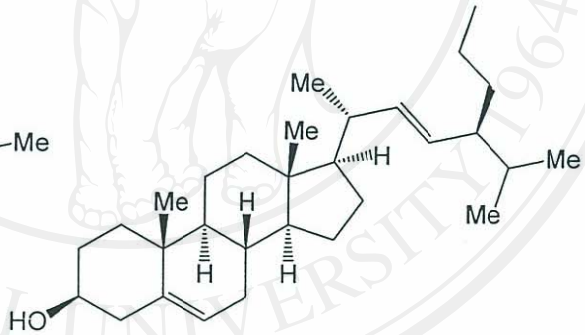

Stigmasterol (**30**)

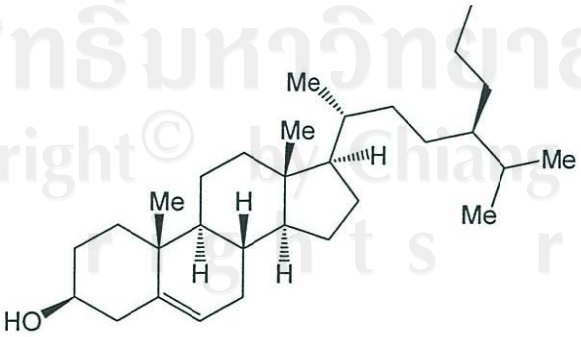

β-Sitosterol (**31**)

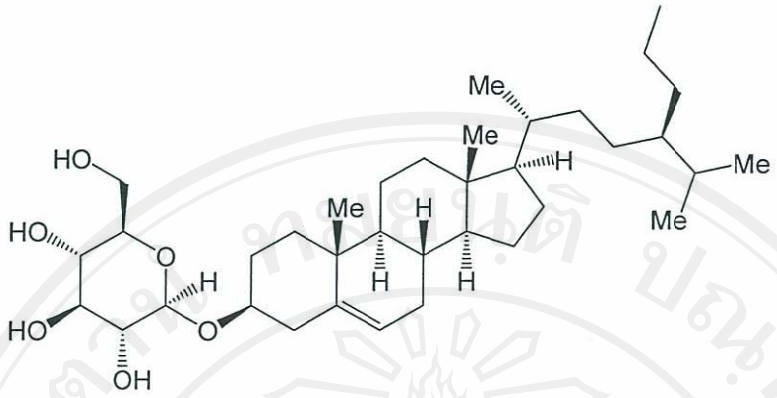

β-Sitosterol glucoside (**32**)

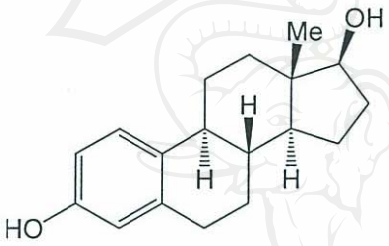

Estradiol (**33**)

Two dihydroxy sterols were isolated from the leaves of *H. indicum* and characterized as 14α-methyl-5α-cholesta-9,24-diene-3β,7α-diol (**34**) and 14α-methyl-24-methylene-5α-cholesta-9,24-diene-3α,7α-diol (**35**) by Srinivas *et al.* in 2002 [40].

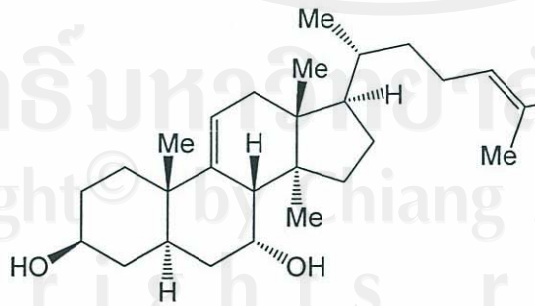

14α-methyl-5α -cholesta-9,24-diene-3β,7α -diol (**34**)

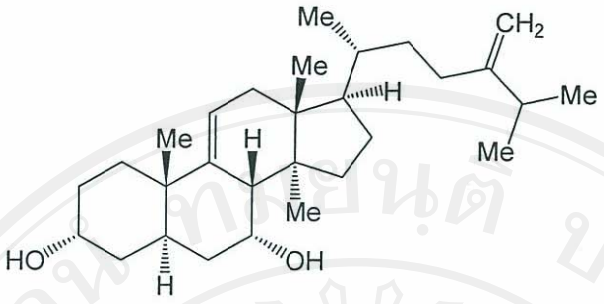

14α-methyl-24-methylene-5α-cholesta-9,24-diene-3α,7α-diol (**35**)

1.2.3 Triterpenoids

The entire plant of *H. indicum* was found to contained chalinasterol (**36**) as reported by Andhiwal in 1985 [5]. In 1996, Pandey *et al.* [31] isolated two triterpenes, lupeol (**37**) and β-amyrin (**38**) from the non-alkaloidal extract of *H. indicum*. Acacic acid lactone (**39**) was isolated from the leaves of this plant by Srinivas *et al.* in 2002 [40].

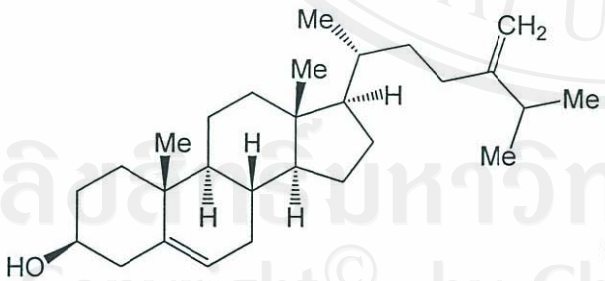

Chalinasterol (**36**)

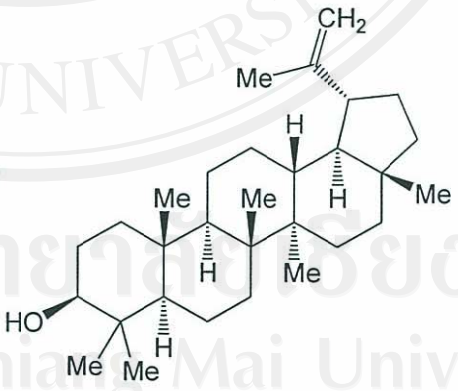

Lupeol (**37**)

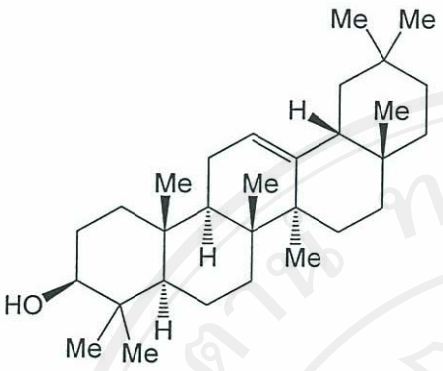

β-Amyrin (**38**)

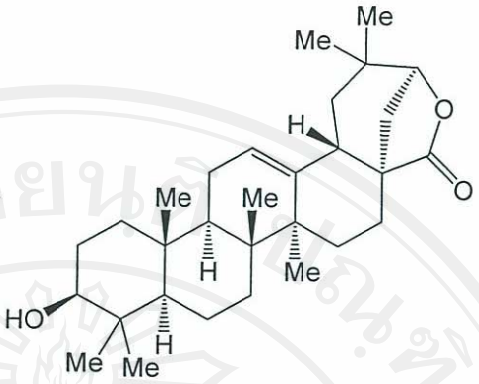

Acacic acid lactone(**39**)

1.2.4 Flavonoids

The first report of the isolation of two flavonoids, 7-hydroxyflavanone (**40**) and naringenin 5-methyl ether (**41**) from the aerial parts of *H. indicum* was revealed by Singh *et al.* in 2003 [37].

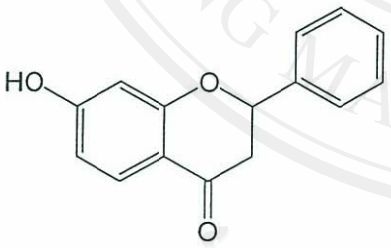

7-Hydroxyflavanone(**40**)

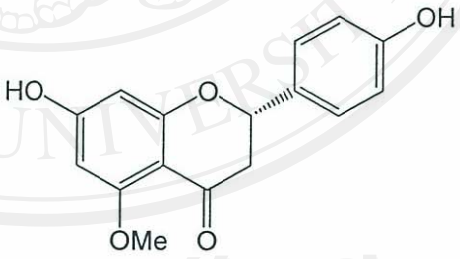

Naringenin 5- methyl ether (**41**)

1.2.5 Miscellaneous Compounds

Quinoid, rapanone (**1**), from entire plant of *H. indicum* was found by Mehta *et al.* in 1981[41]. Hydrocyanic acid (**5**) and hexacosan-1-ol (**6**) were also detected in this plant [5 and 42]. *H. indicum* seeds were found to contain the fatty acid diester of 1-cyano-2-hydroxymethylprop-1-ene-3-ol (**42**) [43].

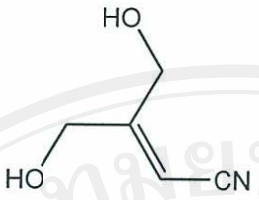

1-Cyano-2-hydroxymethylprop-1-ene-3-ol (**42**)

1.3 Biological Activities for the Extracts of *H. indicum*

The studies of the biological activities of the extracts from *H. indicum* were reported by many researchers which are summarized in Table 2.

Table 2 Biological activities of the extracts from *H. indicum*

Biological Activities	Type of Extract	Plant Part	References
Hepatotoxic activity	Water	Fresh entire plant	[4]
Diuretic activity	Water	Fresh entire plant	[4]
Wound healing acceleration	Water	Fresh entire plant	[4]
	Ethanol	Dried entire plant	[44]
Antifertility effect(unspecified)	Pet-Ether	Fresh entire plant	[5]
Antitumor Activities:-	Water	Dried entire plant	[6]
Leuk-L1210, Leuk-P1534			
Leuk-P388, Melanoma-B16,			
and Sarcoma-WM256(IM)			
Antibacterial activities:-	Methanol	Dried entire plant	[7]
Pseudomonas aeruginosa,			
Stephylococcus aureus,			
Salmonella typhi, and			

Table 2 Biological activities of the extracts from *H. indicum* (continued)

Biological Activities	Type of Extract	Plant Part	References
Escherichia coli	Water	Fresh leaves	[8]
Antifungal Activity:-			
Fusarium oxysporum f.sp. lentis	Water	Fresh leaves	[9, 45]
Uterine stimulant effect	95% Ethanol	Fresh leaves	[45]
Smooth muscle relaxant activity	95% Ethanol	Dried root	[10]
Antispasmodic activity (unspecified type)	Water	Dried seed	[11]
Hypotensive activity	Water	Dried seed	[11]
Anti-inflamatory activity	Water	Dried leaves	[46]

1.4 The Scope and Aims of This Part of the Research

Since, no chemical investigations of the volatile oil and non-polar solvent extracts from the aerial parts of *H. indicum* have been reported. In this research work, we now describe the GC-FID and GC-MS analysis of the volatile compounds and the methyl esters of the major free fatty acids isolated from the hexane extract of this plant as well as their biological activities. The components were analysed by a comparison of mass spectra with literature data (NIST, NISTREP) and by comparison of their programmed-temperature Kováts retention indices (RIs) with those of authentic compounds or with those reported in the literature. [74-76].

1.5 Kováts Retention Index Systems [47-49]

GC retention data are useful for the identification of samples which the components are known. A great amount of retention data such as retention time, relative retention (R_x) or theoretical nonane methods are available for various stationary phases and components but there are great drawbacks in identification as well. In 1958, the first index by Kováts was reported but it found little acceptance during its first decade due to its publication in German. After its publication and previously published papers summarized in English, the uses of retention index became widespread.

The Kováts retention index equation (1.1) is based on the retention of *n*-alkanes with an even number of carbon atoms [50]

$$I_s\,(T°C) = 200\left[\frac{\log X_s - \log X}{\log X_{(Z+2)} - \log X}\right] + 100Z \quad \text{.....(1.1)}$$

Where; I = retention index

s = the compound of interest

X_s = retention time of the interested compound

X = retention time of *n*-alkane

Z, Z+2 = *n*-alkanes with Z and Z+2 carbon atoms, respectively, where Z is an even number

In addition to the above retention system derived by Kováts, the retention index value of a substance is defined according to equation 1.2 [51]

$$I = 100Z + 100\left[\frac{\log t'_{R(x)} - \log t'_{R(Z)}}{\log t'_{R(Z+1)} - \log t'_{R(Z)}}\right] \quad \text{.....(1.2)}$$

$t'_{R(X)}$ = retention time of interested compound

$t'_{R(Z)}$, $t'_{R(Z+1)}$ = retention time of *n*-alkane with Z and Z+1 carbon atoms, respectively.

The retention index of any substance is equivalent to 100-times the carbon number of a hypothetical *n*-alkane with the same adjusted retention time. The Kováts retention index is a useful tool for the comparison of retention data obtained by various authors under different conditions, as it is nearly independent on many of the parameters and conditions of the gas chromatographic analysis.

The temperature dependence of retention index value is a hyperbolic function [49,52-54] described by an Antoine type function, equation (1.3)

$$I(T) = \frac{A + B}{T + C} \quad \text{.....(1.3)}$$

Where I(T) = retention index

T = column temperature, K

A, B and C = experimentally derived constants

Tidor [55-57] has reported the analysis of equation for temperature dependence of retention index by using perfumery compounds on a SE-30 glass capillary column. Both the liner and hyperbolic functions were compared. The linear

equations for retention index against t (°C) or 1/T (K^{-1}) are valid for more or less extended temperature range and varieties of solutes and stationary phases [54]. The investigation of the retention index (I) vs. temperature (t) plots also gives rise to certain general rules. It was seen that on squalane and with *iso*-paraffin samples, the greater substitution in the molecule the greater the greater the influence of temperature on the I value. The values of cyclo-paraffin and aromatics are much more temperature dependent than the I of iso-paraffin [55].

For mixtures of wide boiling point range the determination of retention indices under isothermal conditions would be time consuming and not practical. Van den Dool and Kratz [58] have developed a temperature programmed retention index (I_{TPRI}) using gross retention time instead of log t'_R, as shown in equation (1.4). This equation is valid under linear temperature programmed conditions.

$$I = 100Z + 100\left[\frac{t_{R(X)} - t_{R(Z)}}{t_{R(Z+1)} - t_{R(Z)}}\right] \qquad \text{.....(1.4)}$$

Where Z, Z+1, and Z+2 are alkanes containing Z, Z+1 and Z+2 carbon atom, respectively.

The difficulties have been experienced with the use of *n*-alkane standards, particularly with polar stationary phases and some detectors. The dominant reference series are PAHs, PCBs and *n*-haloalkanes. A review on reference series has been presented [59]:

In the PAHs series [60, 61], naphthalene, phenanthene, chrysene and picene were assigned values of I = 200, 300, 400 and 500, respectively. The PAHs index has

been applied to a considerable number of related studies, including, diesel particle matter [62], coal extracts [63], sediments, and biomedical tissue [64].

The PCBs index has also been studied and used for the identification of PBC compounds [65-67]. The detector that widely used for PBCs and halogenated alkanes was electron capture detector (ECD) [59, 68-70].

When the retention index of a substance is unknown and the substance is unavailable for measurement, its retention index can be estimated. The partial indices for the carbon skeleton and functional groups are summed, making allowances where necessary for the second order interactions between functional groups [54].

Retention index systems are not commonly used in liquid chromatography. The relationships among the retention index, moblil phase and temperature are complex [71]. For reversed phase LC [72], including *n*-alkanes alkyl benzenes, alkane-2-ones, esters and PAHs have been compared and reviewed. The retention index system for identification of toxicologically drug screening is primarily used in HPLC as well as in GC [73].

CHAPTER 2

RESULTS AND DISCUSSION

2.1 Identification of Essential Oil of *H. indicum*.

The essential oil obtained from the aerial parts of *H. indicum* was analyzed by means of GC-FID and GC-MS. Identification of the oil components was performed by a comparison of mass spectra with literature data (NIST, NISTREP) and by comparison of their programmed-temperature Kováts retention indices (RIs) with those of authentic compounds or with those reported in the literature. [74-76].

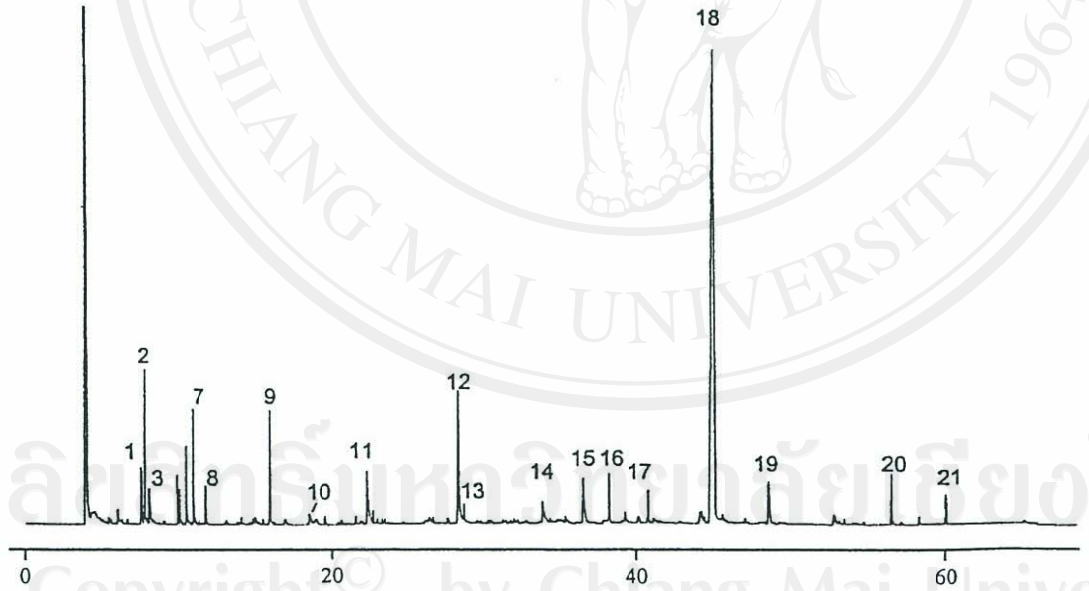

Figure 2 Gas chromatogram of the essential oil of *H. indicum*. See experimental for GC conditions and Table 3 for peak identifications.

Sixteen components were identified and are listed in the order of their elution on the BP5 capillary column used for GC-FID analysis (Table 3) A typical gas chromatogram of the essential oil from *H. indicum* is presented in Figure 2.

Table 3 Volatile components from the aerial part of *H. indicum*.

Peak No.	Compounds	RA[a](%)	RI[b](Exp)	RI[c] (Lit)	MWt	Identification[e]
1	Unidentified	1.6	853			
2	Mixture of :	4.0				
	hexenol and		862	851[T]	100	1,2
	dimethylpentanol				116	2
3	1-Hexanol	1.9	873	867[T]		1,2
4	Unidentified	0.8	936			
5	Unidentified	1.1	940			
6	Unidentified	2.2	954			
7	Unidentified	2.2	968			
8	Unidentified	1.4	997			
9	β-Linalool	3.0	1105	1098[T]	154	1,2
10	Borneol	0.4	1173	1165[T]	154	1,2
11	1-Decanol	1.2	1280	1272[T]	158	1,2
12	1-Dodecanol	6.4	1482	1473[T]	186	1,2
13	β-Ionone	0.6	1493	1485[T]	192[d]	1,2
14	1-Tetradecanol	1.6	1683	1676	214	2
15	1-Pentadecanol	2.6	1785	1778[T]	228	1,2
16	2-Pentadecanone	1.7	1847		226	2
17	Possibly an isomer of phytol	1.0	1950			2
18	Phytol	49.1	2132	1949[T] 2113[T,f]	296[d]	2,3
19	Mixture of :	2.3				
	tricosane and		2300	2300[T]		2,3
	tricosene					
20	*n*-Heptacosane	1.6	2700		380	3
21	*n*-Nonacosane	0.9	2900		408	3

[a] RA, relative area (raw peak area relative to total peak area).
[b] RI (Exp), programmed temperature retention indices as determined on BP5 column using a homologous series of *n*-alkanes (C_8-C_{30}) as internal standard and H_2 as carrier gas.
[c] RI (Lit), values from literature data using He as carrier gas; [T] programmed temperature values. MWt, molecular weight.
[d] confirmed from GC-MS (CI) data.
[e] 1, based on retention index; 2, based on comparison of mass spectra with literature data (NIST, NISTREP) or authentic sample; 3, retention time identical to authentic compound.
[f] RI values from reference [76]

The most prominent compounds found were phytol (49.1%), 1-dodecanol (6.4%) and β-linalool (3.0%) respectively, with integrator raw peak area expressed as

a percentage of the total chromatographable components of the essential oil. These compounds accounted for approximately 87.6% of total essential oil components. A number of components could not be identified due to the lack of reference spectra and/or their relatively low abundance. The major component, phytol, was identified by comparison of its mass spectrum and retention time with those of an authentic sample obtained from BDH. It should be noted that the experimental RI values for compounds 2-15 were systematically higher than the literature values by 6-11 index units. This is probably due in part to a combination of using H_2 as carrier gas, and the use of a retention gap for the GC-FID analysis. The chemical structures of some identified components from the essential oil are shown in Figure 3.

Preliminary testing showed the volatiles oil of *H. indicum* had significant antituberculosis activity against *Mycobacterium tuberculosis* H37Ra in the Alamar blue assay system with MIC of 20.8 μg/mL (average of three determinations). The standard drugs were isoniazide and kanamycin.

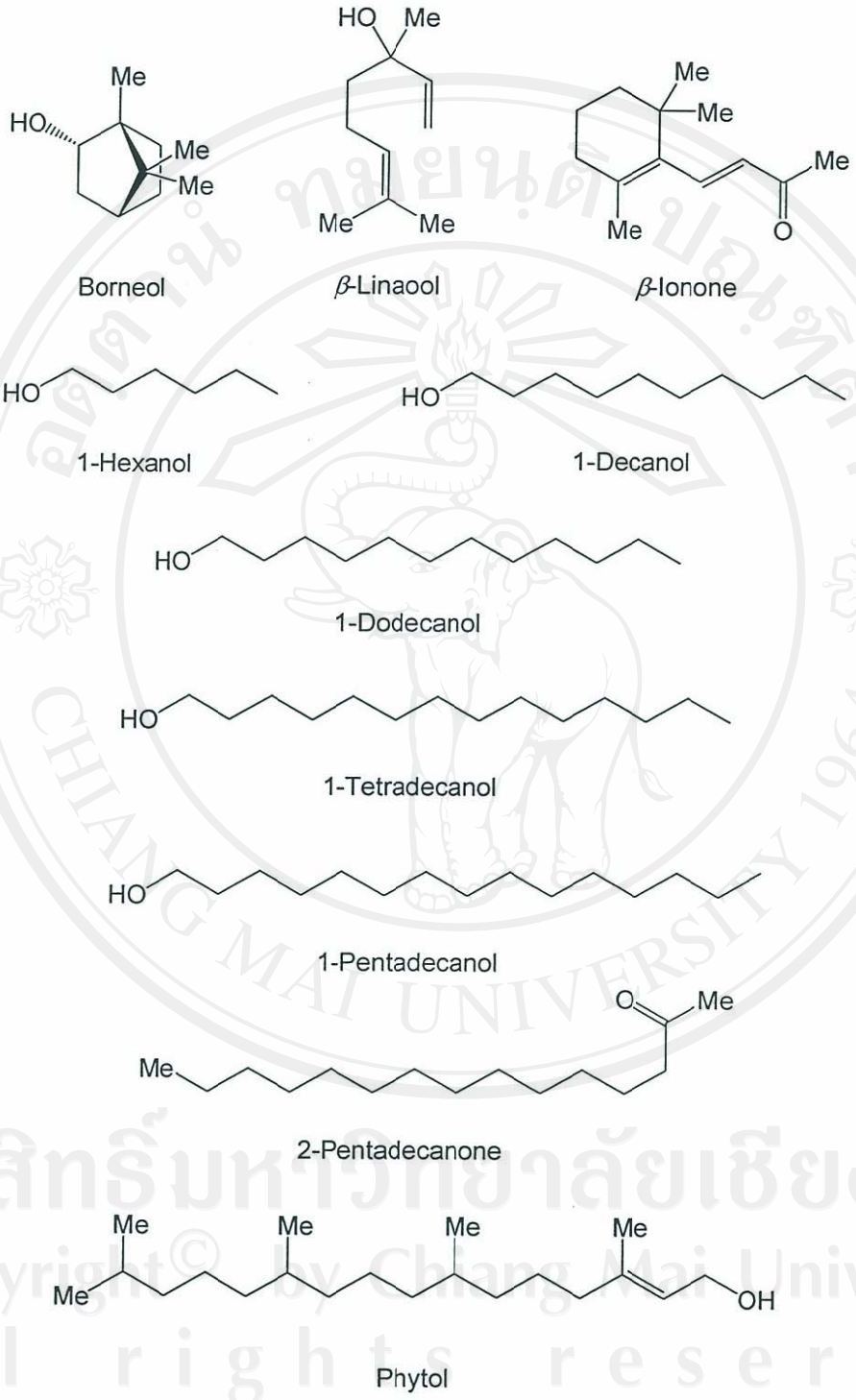

Figure 3 The structures of some identified components of the essential oil from *H. indicum*

2.2 Identification of Free Fatty Acids from the Hexane Extract of *H. indicum*

When the crude hexane extract from the aerial parts of *H. indicum* was analyzed by direct insertion mass spectrometry (DI-MS) the presence of at least eleven fatty acids were indicated based upon fragment-ion (EI mode) and molecular weight (CI mode) information. Determination of percentage composition of the crude hexane extract and identification of the fatty acids were performed by conversion to their methyl esters using the methylation protocol of Bannon *et al.* [77] followed by GC-FID and GC-MS analysis. The methyl esters were identified by their RI values and a comparison of their mass spectra with literature data (NIST, NISTREP).

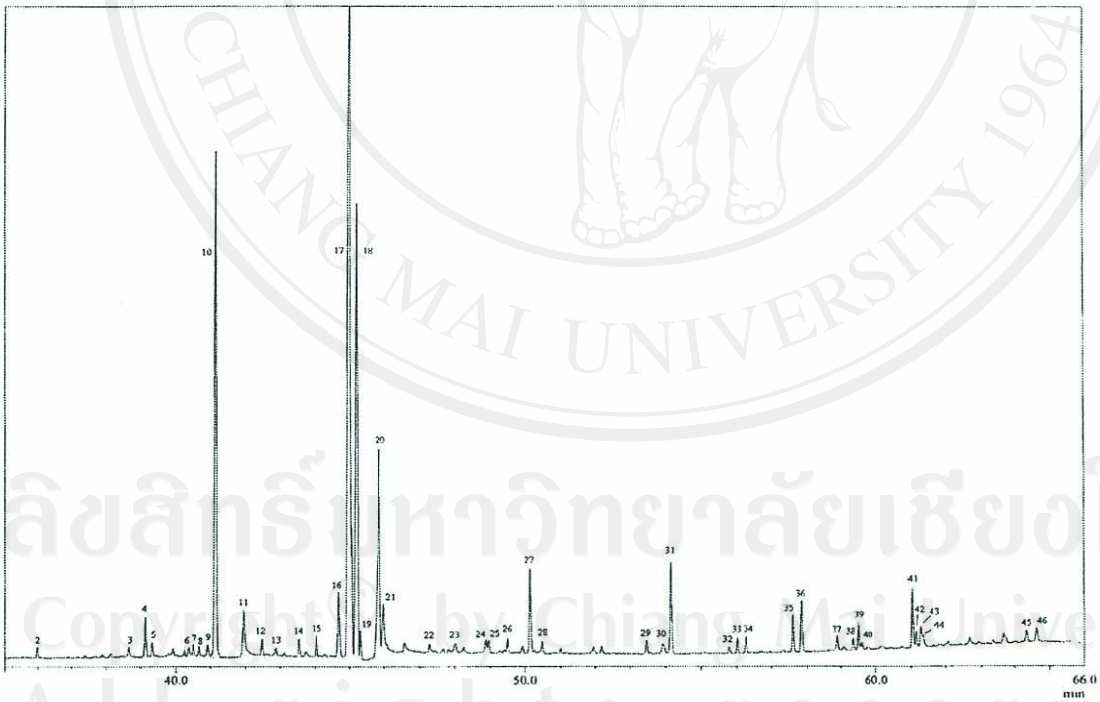

Figure 4 TIC profile of the methylated crude hexane extract from the aerial parts of *H. indicum.* See experiment for GC-MS conditions and Table 4 for peak identifications.

Table 4 Chemical components found in the crude hexane extract of *H. indicum* after methylation.(Peak numbers refer to TIC of Figure 4)

Peak number	MS library match	MW	RI [a] (exp)	RI[b] (lit.)	RA[c] (%)	RA[d] (%)
2	tetradecanoic acid, methyl ester	228	1708	1707	0.3	0.5
3	pentadecanoic acid, methyl ester	242	1808		0.2	Tr
4	6,4,10-trimethyl-2-pentadecanone	268	1828		1.0	ND
6	3,7,11,15-tetramethyl-2-hexadecen-1-ol	296	1878		0.3	ND
7	9-hexadecenoic acid, methyl ester	268	1883	1886	0.4	ND
10	hexadecanoic acid, methyl ester	270	1910	1909	16.1	14.2
11	hexadecanoic acid	256	1947*	1939	1.5	ND
14	heptadecanoic acid, methyl ester	284	2009		0.4	Tr
17	9,12-octadecadienoic acid, methyl ester	294	2073	2074	29.8	39.7
18	9-octadecenoic acid, methyl ester	296	2082	2082	16.3	32.4
20	octadecanoic acid, methyl ester	298	2110	2109	9.2	5.1
21	octadecenoic acid	282	2116		2.0	ND
23	nonadecanoic acid, methyl ester	312	2209		0.2	Tr
27	eicosanoic acid, methyl ester	326	2311	2312	2.4	0.7
30	*n*-pentaeicosane	352	2500		0.4	ND
31	docosanoic acid, methyl ester	354	2512		2.6	0.5
32	*n*-hexaeicosane	366	2600		0.2	Tr
33	tricosanoic acid, methyl ester	368	2612		0.5	Tr
35	*n*-heptaeicosane	380	2700		1.0	Tr
36	tetracosanoic acid, methyl ester	382	2714		1.5	0.5
38	*n*-octaeicosane	394	2800		0.3	Tr
40	pentacosanoic acid, methyl ester	396	2809		0.2	Tr
41	*n*-nonaeicosane	408	2900		1.7	Tr
43	hexacosanoic acid, methyl ester	410	2908		0.6	0.6
45	hentriacontane	437	3100		0.4	Tr
46	octacosanoic acid, methyl ester	438	3107		0.5	0.4

[a] RI(exp): programmed temperature retention indices as determined on BP-1 column using a homologous series of *n*-alkanes (C_8-C_{30}) as internal standard and He as carrier gas.

[b] RI(lit.): programmed temperature retention indices from the literature [78] using He as carrier gas.

[c] RA: % TIC area (raw peak area relative to total TIC area).

[d] RA: % GC-FID area (raw peak area relative to total peak area); Tr : Trace (<0.1%); ND : Not detected.

* Confirmed by comparison with hexadecanoic acid standard analysed under identical conditions.

Sixteen fatty acids were identified as their methyl esters are listed in the order of their elution on the capillary column used for the GC-MS analysis (Table 4). The percentage composition values were obtained from GC-FID integrator data, assuming equal relative FID response, and showed that the fatty acids comprise 95% of the chromatographable components of the crude extract with 9,12-octadecadienoic acid, (39.7%), 9-octadecenoic acid (32.4%), hexadecanoic acid (14.2%) and octadecanoic acid (5.1%), as the major constituents. The GC-MS total-ion current (TIC) profile of the methylated fatty acids from *H. indicum* is presented in Figure 4 and forty six compounds were detected during the mass-spectrometric analysis. Twenty six of these compounds account for 90% of the TIC. The major components comprise fatty acids with a small amount of 6,10,14-trimethyl-2-pentadecanone and 3,7,11,15-tetramethyl-2-hexadecen-1-ol, as well as a homologous series of *n*-alkanes present at trace level and ranging from C_{25} to C_{31} also found (see Table 4). In Table 4 the TIC integrator raw peak area for each component is expressed as a percentage of the total TIC raw area for the chromatographable components of the methylated extract. A number of components (with collective peak area accounting for ca. 10%) could not be identified in the TIC due to the lack of reference spectra and/or their relatively low abundance and are not listed in Table 4.

Although the GC-FID analysis showed peaks in the chromatogram for only the relatively abundant fatty acids, the presence of other *n*-alkanoic acids, some present at trace level, was inferred from minor peaks in the TIC and their coincidence with a plot of MS fragment ions characteristic for their methyl esters (*m/z*: 74 and 87). Their presence was confirmed and their identity verified by further mass-spectral evidence and the fact that their calculated RI values corresponded to those obtained for the

appropriate methyl ester homologue from the least-squares equation of the RI values generated from the more abundant acids.

The MS fragment ion plot for all of the *n*-alkanoic acid esters shows a profile extending over the carbon number range C_{14} to C_{28} with pronounced even over odd carbon number preference (CPI) characteristic of epicuticular waxes derived from the leaves of terrestrial higher plants [79].

Preliminary biological testing showed that the crude hexane extract of *H. indicum* had modest antituberculosis activity against *Mycobacterium tuberculosis* H37Ra in alamar blue assay system with a MIC of 100 μg/mL.

CHAPTER 3

CONCLUSIONS

Heliotropium indicum Linn. has been used as a component of traditional medicines for several medical applications in a number of countries, however little scientific evidence has supported their effectiveness. Preliminary bioassay in this work revealed that the volatile oil and hexane extract from this plant had significant antituberculosis activity against *Mycobacterium tuberculosis* H37Ra in the Alamar blue assay system with the MIC of 20.8 μg/mL (average of three determinations, 12.4, 25, and 25 μg/mL, respectively) and 100 μg/mL, respectively.

The essential oil from the aerial part of *H. indicum*, collected from Teng Nam Village, Muang District, Phitsanulok, Thailand, in February 2003, was isolated by hydrodistillation and analyzed by means of GC-FID and GC-MS. The essential oil was obtained in 0.004% yield as a light brown liquid. The major components of this volatile oil were identified as phytol (49.1%), 1-dodecanol(6.4%), *β*-linalool (3.0%), 1-pentadecanol (2.6%), 1-hexanol (1.9%),2-pentadecanone (1.7%), 1-tetradecanol (1.6%), *n*-heptacosane (1.6%), 1-decanol (1.2%), *n*-nonacosane(0.9%), *β*-ionone (0.6%) and borneol (0.4%).

The crude hexane extract from the aerial parts of *H. indicum* was analyzed by direct insertion DI-MS the presence of at least eleven fatty acids were obtained based upon fragment-ion (EI mode) and molecular weight (CI mode) information. The analysis of the crude hexane extract and the identification of fatty acids were performed by conversion to their methyl esters followed by GC-FID and GC-MS

analysis. Sixteen fatty acids were identified as their methyl esters. The percentage composition values were obtained from GC-FID integrator data and showed that the fatty acids comprise 95% of chromatographable components of the crude extract with 9,12-octadecadienoic acid (39.7%), 9-octadecenoic acid (32.4%), hexadecanoic acid (14.2%), octadecanoic acid (5.1%), eicosanoic acid (0.7%), hexacosanoic acid (0.6%), tetradecanoic acid (0.5%), docosanoic acid (0.5%), tetracosanoic acid (0.5%), and octacosanoic acid (0.4%) as the major components.

During the mass-spectrometric analysis, 46 compounds were detected from the GC-MS total-ion current (TIC) profile of the methylated fatty acids. Twenty six of these compounds account for 90% of the TIC. The major components comprise fatty acids, 9,12-octadecadienoic acid (29.8%), 9-octadecenoic acid (16.3), hexadecanoic acid (16.1% and 1.5%), octadecanoic acid (9.2%), docosanoic acid (2.6%), eicosanoic acid (2.4%), octadecenoic acid (2.0%), tetracosanoic acid (1.5%), hexacosanoic acid (0.6%), octacosanoic acid (0.5%), tricosanoic acid (0.5%), tetradecanoic acid (0.3%), pentadecanoic acid (0.2%), pentacosanoic acid (0.2%), nonadecanoic acid (0.2%), with a small amount of 6,4,10-trimethyl-2-pentadecanone (1.0%) and 3,7,11,15-tetramethyl-2-hexadecen-1-ol (0.3%), as well as a homologous series of *n*-alkanes present at trace level and ranging from C_{25} to C_{31} were also found.

CHAPTER 4

EXPERIMENTAL

4.1 Source and Authentication of the Plant Materials

The fresh aerial parts of *H. indicum* were collected from Teng Nam Village, Muang District, Phitsanulok, Thailand, in February 2003. The plant was identified as *Heliotropium indicum* Linn. by comparison with the herbarium specimens at the herbarium of the Faculty of Pharmacy, Chiang Mai University, Thailand. The voucher specimen (No. 003463) was deposited in the herbarium of Department of Pharmaceutical Sciences, Faculty of Pharmacy, Chiang Mai University, Thailand.

4.2 Analysis of Essential Oil

Fresh plant material (30 kg) was chopped into small pieces and then subjected to hydrodistillation for 5 h, using a modified Clevenger-type apparatus to yield 1.20 g (0.004%) of a light brown oil. The essential oil was dissolved in methylene chloride and dried over anhydrous sodium sulfate. In this study, we have used gas chromatography - flame ionization detector (GC-FID) and gas chromatography-mass spectrophotometry (GC-MS) analysis, to identify and determine the composition of this essential oil. The GC-FID analysis was carried out using a Varian 3700 gas chromatograph coupled to Shimadsu C-R3A integrator. Separation was achieved using H_2 as carrier gas (ca. 1 mL/min) with fused silica capillary column (25QC/BP5) obtained from SGE, Australia (25 m × 0.25 mm i.d., 0.25 μm film thickness). The capillary column was connected to a Z guard column (2 m) of deactivated fused silica supplied by Phenomenex. Injector and detector temperatures were 260°C and 280°C,

respectively; oven temperature programme, 2 min isothermal at 40°C, rising at 4 °C/min to 280°C (4 min isothemal). Programme-temperature Kováts retention indices (RI) were obtained by GC-FID analysis of an aliquot of the essential oil spiked with an *n*-alkane mixture containing each homologue from *n*-C_8 to *n*-C_{30}. The GC-MS analysis was performed in both electron impact (EI, 70 eV) and chemical ionization mode (CI, *iso*-butane reagent gas) with a Shimadzu QP5000 system, using He as the carrier gas and a capillary column (BPX5) supplied by SGE, Australia (30 m × 0.32 mm i.d., 0.25 μm film thickness). Gas chromatographic conditions were as above, with a He flow rate of 1.4 mL/min.

4.3 Extraction and Identification of Fatty Acids

The complete fresh aerial parts (20 kg) of *H. indicum* were air-dried and ground giving a powdered material (2.5 kg). This material was extracted by soaking in hexane at room temperature for 2 weeks with three changes of hexane (1 × 3 L, 2 × 2 L). The resultant extracts were combined and concentrated under a vacuum to yield a dark green gum (27.67 g).

Initial analysis of this extract was performed using direct insertion mass spectrometry (DI-MS) and both chemical ionisation (CI: *iso*-butane reagent gas) and electron impact (EI) modes.

4.3.1 Methylation of Fatty Acids

The methylation procedure was based on the protocol of Bannon [77]. The crude hexane extract (50 mg) was transferred into a 50-mL long neck round bottom flask. The mixture was boiled under reflux for 3 min with 5 mL of methanolic

potassium hydroxide solution. The 1 mL of 50% boron trifluoride-methanol complex was added and the mixture was boiled under reflux for a further 2 min stopped heating, then 4 mL of isooctane and approximately 15 mL of saturated sodium chloride were added and the flask was closed and shaken vigorously for 30 sec while tepid. The liquid level was brought to the neck of the flask with more sodium chloride solution and the phases were allowed to separate and 1 μL of the upper layer was analyzed by GC-FID and GC-MS.

4.3.2 GC-FID and GC-MS Analysis

GC-FID analysis was carried out using a Varian 3700 gas chromatograph coupled to a Shimadsu C-R3A integrator. Separation was achieved using H_2 as carrier gas (ca. 1 mL/min) with a fused silica capillary column (25QC/BP5) obtained from SGE, Australia (25 m × 0.25 mm i.d., 0.25 μm film thickness). The capillary column was connected to a Z guard column (2 m) of deactivated fused silica supplied by Phenomenex. Injector and detector temperatures were 260°C and 280°C, respectively; oven temperature programme, 2 min isothermal at 40°C, then at 4°C/min to 280°C (10 min isothermal).

GC-MS analysis was performed in electron impact mode (EI, 70 eV) with a Shimadzu QP5050A system, using the same temperature programme, with He as the carrier gas (1 mL/min) and a capillary column (BP1) supplied by SGE, Australia (30 m × 0.32 mm i.d., 0.25 μm film thickness). For each analysis, programmed-temperature Kováts retention indices (RI) were obtained by analysis of an aliquot of the methylated extract spiked with an *n*-alkane mixture containing each homologue from *n*-C_8 to *n*-C_{30}.

4.4 Antituberculosis Activity

Antimicrobial susceptibility testing was performed in 96-well microplates [80]. Outer perimeter wells were filled with sterile water to prevent dehydration in experimental wells. Initial screened-sample dilutions were prepared in either dimethyl sulfoxide or distilled deionized water. The dissolved-screened samples were then diluted by Middlebrook 7H9 media containing 0.2% v/v glycerol and 1.0 g/L casitone (7H9GC), and subsequent two fold dilutions were performed in 0.1 mL of 7H9GC in the microplates. Frozen inocula (*M. tuberculosis* H37Ra) was grown in 100 mL of 7H9GC containing 0.005% Tween 80. Culture was incubated in 500 mL plastic flask on rotary shaker at 200 rpm and 37°C until they reached an optical density of 0.4-0.5 at 550 nm. Bacteria were washed and suspended in 20 mL of phosphate buffered saline and passed through an 8-m-pore-size filter to eliminate clumps. The filtrates were aliquoted, stored at -80°C) were diluted 1: 100 in 7H9GC. Addition of 0.1 mL to a well resulted in final bacterial titers of about 5×10^4 CFU/mL. Wells containing sample only were used to determine whether the tested-samples themselves could reduce the dye or not. Additional control wells consisted of bacteria only (B) and medium only (M). Plates were incubated at 37°C. Starting at day 6 of incubation, 20 μL of Alamar Blue solution and 12.5 μL of 20% Tween 80 were added to one B well and one M well, and plates were reincubated at 37°C. Wells were observed at 24 h for a colour change from blue to pink. If the well remained blue, additional M and B well were tested daily until a colour change occurred, at which time reagents were added to all remaining wells. Plates were then incubated at 37°C, and results were recorded at 24 h post-reagent addition. Visual MICs were defined as the lowest concentration of sample that prevented a colour change.

PART II

ASYMMETRIC SYNTHESIS OF (+)-CASTANOSPERMINE

CHAPTER 1

INTRODUCTION

The total synthesis of natural products requires selective methods to adapt to the structural complexity that Nature has introduced into natural compounds. From this challenge derives the impetus to find new reactions, new reagents and new catalysts to run reactions in a chemoselective, regioselective and stereoselective way. Recently, multicomponent, combinatorial or enzymatic processes have expanded the synthetic tools available to researchers, and topics like atom-economy and environmentally friendly syntheses became the concern of organic chemists. In this thesis we have approached the synthesis of the natural product and glycosidase inhibitor, castanospermine, (1*S*, 6*S*, 7*R*, 8*R*, 8a*R*)-tetrahydroxyoctahydroindolizidine (**1a**). This natural product belongs to the class of indolizidine alkaloids, which are attracting growing interest from synthetic chemists for their various and essential biological activities.

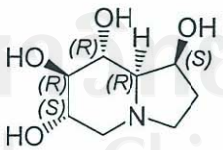

(+)-Castanospermine (**1a**)

Figure 5 Structure and stereochemistry of (+)-castanospermine (**1a**)

1.1 Indolizidine Alkaloids

Indolizidines are widely distributed in both plants and animal. Their structures can be described as either derivatives of the aromatic bicyclic indolizine or as 1-*aza*-bicyclo[4.3.0]octane (Figure 6) .

The indolizidine alkaloids display a wide range of biological activities [81-83] and have been the subject of numerous synthetic studies [82, 84-109]. The development of general methods for the synthesis of racemic and enantiopure indolizidines remains an area of active investigation.

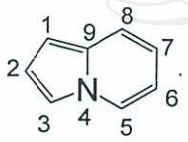

Indolizine

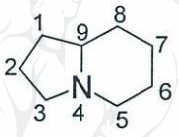

Azabicyclo[4.3.0]octane

Figure 6 The parent structures of bicyclic of indolizidine alkaloids

Most of the naturally occurring indolizidines have been isolated from species of the genus *Dendrobates* (poison-arrow frogs), *Monomorium* (ants), *Dendrobium* (orchids), *Tylophora* and the *Leguminosae* family (plants). The classification of the indolizidines according to their natural sources is difficult due to the structural diversity within these species. Nevertheless some characteristic structural motives are unique for the species and are often linked to the high biological activities of the compounds. Among them the hydrophilic polyhydroxy indolizidines and lipophilic pumiliotoxins are the two most important classes of compounds.

1.2 Polyhydroxylated Indolizidines

A variety of alkaloids possessing a polyhydroxylated indolizidine structure have been isolated from natural sources, including plants and microorganisms. Some of them are excellent inhibitors of biologically important pathways, including the binding and processing of glycoproteins and show potent glycosidase inhibitory activities [110-118]. Among naturally occurring polyhydroxylated indolizidines, lentiginosine (**2**) (an amyloglycosidase inhibitor) [119-125] swainsonine (**3**) (a potent and specific inhibotor of lysosomal and glycoprotein processing α-mannosidases) [46-49], castanospermine (**1a**) (a potent inhibitor of α-glucosidases including lysosomal and glycoprotein processing enzymes) [130,131], and uniflorine A (**4**) (a potent inhibitor of the α-glucosidases, maltase and sucrase) [132] have attracted the greatest attention from both synthetic and biological points of view and represent good examples of dihydroxylated, trihydroxylated, tetrahydroxylated and pentahydroxylated indolizidines, respectively (Figure 7).

To find structure-activity relationships, this interest has been extended to the synthesis of stereoisomers and analogues. Although in some cases there is close structure resemblance between the biologically active indolizidine and the natural sugar substrate, in many cases this resemblance does not exist.

For instance, swainsonine, which is one of the strongest α-D-mannosidase inhibitors, lacks any significant resemblance with mannose. Since the structure-activity relationships in indolizidines are not straightforward, many stereoisomers and analogues have been synthesized and their biological activities tested. These analogues have been used as biological tools and have been examined as chemotherapeutic agent for diabetes [133-136], cancer [137], and HIV [138-141].

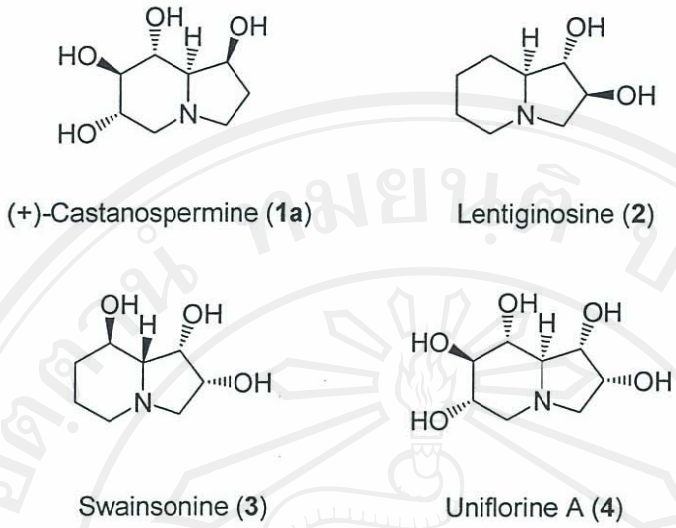

Figure 7 Representative examples of glycosidase inhibitors with the structure of poly hydroxylated indolizidines.

Their biological activity is believed to be a result of their ability to mimic the transition state involved in substrate hydrolysis. For example, the activity of castanospermine against glycosidase has been tied to the similarity of the six-membered ring to the glycosyl cation [141]. In the less obvious way, the anti-mannosidase activity of swainsonine has been related to the resemblance of the five-membered ring to the mannosyl cation [142]. It has been suggested that their rigid, bicyclic structures are responsible for their potent activity [143]. Due to their vicinal polyhydroxylated structure, most of the reported syntheses of castanospermine, swainsonine and analogues employ natural sugars as starting materials.

1.3 Castanospermine and Stereoisomers

Castanospermine (**1a**) is a polyhydroxylated indolizidine alkaloid that has a molecular formula of $C_8H_{15}N_1O_4$ and is known by many names such as 1,6,7,8–tetrahydroxyoctahydroindolizidine; 1,6,7,8-tetrahydroxyoctahydrolizine; (1*S*, 6*S*, 7*R*, 8*R*, 8a*R*)-1,6,7,8-tetrahydroxyindolizidine; octohydro-1,6,7,8-indolizinetetrol; 1,6,7,8-indolizinetetrol and castanospermine.

Castanospermine has five chiral carbons (1, 6, 7, 8 and 8a) and a total of 31 stereoisomers, but only nine, (+)-castanospermine **1a**, (-)-castanospermine **1b**, (+)-1-epicastanospermine **1c**, (-)-1-epicastanospermine **1d**, (+)-6-epicastanospermine **1e**, 1,6-diepicastanospermine **1f**, 6,7-diepicastanospermine **1g**, 6,8a-diepicastanospermine **1h** and 8a-epicastanospermine **1i**, have been synthesized (Figure 8). Some of these were made by design, while others were discovered as by-products of reactions synthesizing the main product. Some pathways to making these isomers use hexose derivatives which already contain 4 of the 5 desired chiral centers since making them from smaller fragments is a long process.

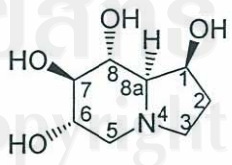

1a

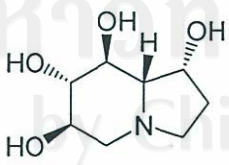

1b

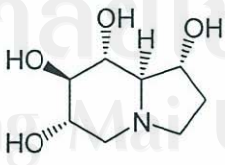

1c

Figure 8 Structures of (+)-castanospermine (**1a**) and its synthesized epimers

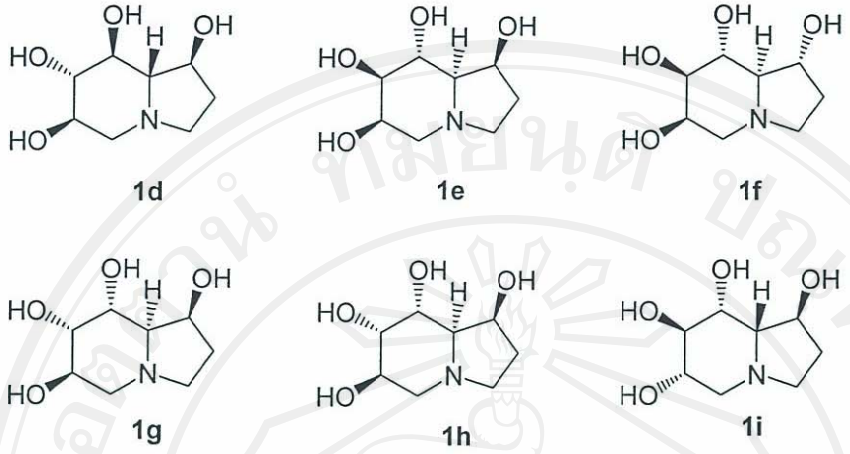

Figure 8 Structures of (+)-castanospermine (**1a**) and its synthesized epimers (continued.)

1.3.1 Natural Occurrences and Isolation of Castanospermine

Castanospermine (**1a**) which occurs in the seeds of *Castanospermum australe* [130] and also the pods of *Alexa leiopetala* [131], is one of a number of plant derived, polyhydroxylated alkaloids that are glycosidase inhibitors, including swainsonine (**3**), deoxynorjirimycin (**5**) and 2,5-dihydroxymethyl-3,4-dihydroxypyrrolidine, DMDP (**6**).

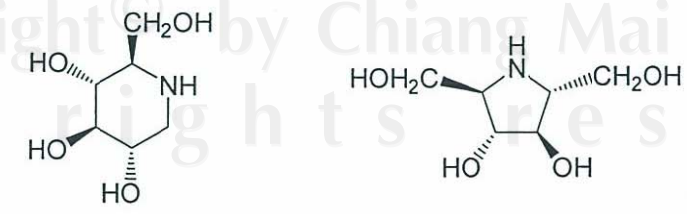

Figure 9 Structure of deoxynorjirimycin (**5**) and DMDP (**6**)

The first reported isolation of castanospermine was on July 29, 1980, in a publication in the journal *Phytochemistry* [130]. In this paper, castanospermine (**1a**) was isolated from a tall chestnut tree, *Castanospermum australe* the only species of the genus *Castanospermum*.

C. australe belongs to the Fabaceae family. It is native to coastal rainforests and beaches in Australia which are found from around Lismore, New South Wales to the Iron Range, Cape York Peninsula on the Queensland coast and 160 km west to the Bunya Mountains.

Figure 10 Distribution areas of *C. australe* in Australia (http://www.anbg.gov.au/gnp/interns-2002/castanospermum-australe.html)

It grows in moist, fertile, well-drained soils on terraces on the side of mountains or along the banks of rivers and streams. The Black Bean tree is also found in New Caledonia and Vanuatu.

C. australe is a tall tree with smooth bark. The leaves are imparipinnate, 30-50 cm long, and the flowers are arranged in racemes usually on the old wood. The large coriaceus pods are 10-35 cm long and contain 3-5 large chestnut-like seeds. The

seeds of this species are frequently eaten by horse and cattle and unripe seeds can cause severe gastrointestinal irritation and sometimes death. The Australian aborigines use them as food after soaking them in water and roasting.

The isolation of castanospermine from the seed of *C. australe* was performed as follows;

The seeds were finely ground and extracted with ethanol, filtered, and then concentrated under reduced pressure. The extract was then applied to a cation exchange column. The column was washed with water, followed by ammonia to elute the amino acids and castanospermine. The solution was concentrated under reduced

Figure 11 Pictures of the leaves, inflorescences and seeds of *C. australe*. (Photographed by D. Greig and J. Wrigley; http://www.anbg.gov.au/gnp/interns-2002/castanospermum-australe.html)

pressure, and diluted with water several times to remove the ammonia. The remaining solution was then applied to a column of Dowex 50 resin in the protonated form and then washed with pyridine to elute the acidic and neutral amino acids. The column was then washed with ammonium to elute the remaining castanospermine followed by arginine. The fractions containing only castanospermine were combined and then concentrated under reduced pressure, yielding a viscous brown syrup. After the syrup had been standing for a while, large cubic crystals formed and were then re-crystallized from ethanol. A colourless crystal of castanspermine was isolated in 0.3% yield from these seeds. Using the method of X-ray crystallography, the relative stereostructure was also determined.

Although castanospermine was initially isolated in *C. australe*, it has since been isolated from the dried pod of a related species called *Alexa leiopetala* (which was collected in 1931 in Guyana but not identified until 1987) and has been tentatively identified in seven other species of this same genus [131]. The seeds of *Alexa grandiflora* contain a higher percent of dry weight of castanospermine (1.39%) than the other plants in which it is believed to be found.

1.3.2 Biological Activities of Castanospermine

The biological properties of castanospermine can be understood in terms of inhibition of the interaction between the glucosyl residue of a glycoconjugate and an enzyme or other protein. Two main factors contribute to this inhibition:

I) The strong structural resemblance between the four substituents at C-6, C-7

and C-8 and C-8a on the piperidine ring of castanospermine and the four substituents on C-2, C-3, C-4 and C-5 of the pyranose ring of D-glucose [143].

II) The metabolic inertness of castanospermine in animal cells.

Glucosyl residues are found in animals in dietary polysaccharides of plant and animal origin, as transient intermediates in the biosynthesis of asparagine-linked glycans of glycoproteins and as constituents of glycosphingolipids, *O*-linked glycans of glycoproteins, glycogen and collagen. It was established soon after its isolation [130] that castanospermine is a potent and specific inhibitor of *α*- and *β*-D-glucosidases from a wide range of organisms and sub-cellular locations *e.g.* lysosomal *α*- and *β*-D-glucosidases [144], glycoprotein processing *α*-D-glucosidases [145], digestive *α*- and *β*-D-glucosidases [146], the broad specificity cytosolic *β*-D-glucosidase [147] and plant thioglucosidase (myrosinase) [148].

Many previous reports revealed that castanospermine was a potent inhibitor of several glucosidases including mammalian intestinal sucrase and glucosidase involved in lysosomal glycoprotein processing. For example, biological activities of castanoapermine have indicated potential utility in the treatment of viral infections [140, 149-160], cancers [161-167], malaria [168] and diabetes [169-171] as well as showing anti-inflammatory [172, 173] and immunosuppressant [174-177] properties.

Recently biological activities showed that the glucosidase inhibitor castanospermine (**1a**) has been found to prevent clinical signs of experimental autoimmune encephalomyelitis (EAE) in SJL/N mice by interfering with signal transduction of the interleukin-2 (IL-2) receptor upon binding to IL-2 [178]. This leads to impaired clonal expansion of T cells, thought to be a crucial phase in the immune attack associated with EAE. The alkaloid's ability to alter glycoprotein

processing seems not to be involved, however, since neither the expression of the highly glycosylated IL-2 receptor nor its ability to bind IL-2 was affected. It also did not induce T cell apoptosis, transendothelial migration of T cells, or expression and function of other molecules involved in endothelial adhesion. This very specific mode of action, coupled with castanospermine's low toxicity, indicates therapeutic potential for the treatment of autoimmune diseases such as multiple sclerosis, for which EAE is a prototypical animal model. In another study with possible therapeutic applicability, castanospermine was found to inhibit the growth of infectious bovine viral diarrhoea virus, an animal model for the hepatitis C virus, in a dose-dependent manner (IC_{50} 47 μM) [179]. Patents on the use of castanospermine esters, in particular Bucast (the 6-*O*-butanoyl ester), for the treatment of diseases caused by viruses such as the hepatitis B and C viruses [180] and the influenza virus [181] are of related interest.

1.3.2.1 Enzymology of Glucosidases

Castanospermine (**1a**) is highly specific for inhibition of α- and β-D-glucosidases. This specificity makes it a useful tool for comparing the kinetics and mechanism of action of different α- and β-D-glucosidases *in vitro* [147, 182]. It has become the yardstick by which novel natural and synthetic α- and β-D-glucosidase inhibitors are judged *e.g.* nectrisine [182] or calystegins [184]. The high affinity of α-D-glucosidases for castanospermine (**1a**) has been exploited in an ingenious manner to isolate liver Golgi endomannosidase by affinity chromatography [185]. Inclusion of castanospermine (**1a**) in the buffer prevented binding of α-D-glucosidases to the α-linked glucosyl residue of the ligand, Glcα1→3Man. The specificity and potency of

castanospermine (**1a**) have also been used to improve the efficiency of an assay for seminal α-D-glucosidase [186].

1.3.2.1.1 Digestive Glucosidases

Consumption of the chestnut-like seeds of the Moreton Bay chestnut *Castanospermum australe* has been reported to lead to gastrointestinal problems and occasional deaths among animals and humans in its native Australia [187]. The cause of death was probably a combination of the effects of castanospermine (**1a**), especially if consumption was prolonged. However, the acute gastrointestinal problems can be attributed to the very potent inhibition of mammalian intestinal disaccharidases by castanospermine (**1a**) with sub micromolar values of K_i for the inhibition of sucrase and maltase. This would lead to decreased absorption of monosaccharides and osmotic diarrhoea [171, 188-191]. The controlled inhibition of the digestion and absorption of dietary carbohydrates in the small intestine has therapeutic potential in the treatment of diabetes and obesity. Castanospermine (**1a**) can delay the hyperglycemic response to oral sucrose in normal and diabetic (streptozoticin-induced) rats [170, 192]. Glucosyl derivatives of castanospermine (**1a**) have been synthesized to obtain selectivity of inhibition of oligosaccharidases, but it has been difficult to predict the specificity of these pseudo-disaccharides [193]. Two other α-D-glucosidase inhibitors, the pseudotetrasaccharide acarbose (BAYg5421) and miglitol ((*N*-hydroxyethyl)-1-deoxynojirimycin, BAY m1099) are in clinical use or undergoing clinical trials for treatment of non-insulin-dependent and insulin-dependent diabetes mellitus [194-196]. Acarbose, unlike miglitol, is not absorbed appreciably into the bloodstream and therefore its action is largely confined to the intestine. Its main side effect is moderate

diarrhoea and associated flatulence. Castanospermine (**1a**) would be expected to cause systemic complications as well as diarrhea because of its absorption into the bloodstream, especially if high concentrations are used.

There are marked differences between species in the specificity of inhibition of digestive disaccharidases by castanospermine (**1a**) [197-204]. For example, castanospermine (**1a**) is a good inhibitor (K_i 0.8 mM) of the soluble midgut trehalase from the larvae of the gypsy moth [201] but it does not inhibit trehalase of the aphid *(Acyrthosiphon pisum,* Harris) [202]. This differential inhibition is potentially the basis of selective insecticides. Interestingly, castanospermine (**1a**) is a very active feeding deterrent to the aphid and to nymphs of the migratory locust, *Locusta migratoria* L but not to nymphs of the desert locust *Schistocerca gregaria* Forsk [203]. This feeding deterrence may not result from inhibition of glycosidases but from recognition of the castanospermine (**1a**) by taste receptors on sensillae on the insect mouthparts, which normally recognize sugars and evoke a response to eat. The molecular basis of this signaling is under investigation as it offers the possibility of crop protection. This property of castanospermine (**1a**) and certain other naturally occurring aminosugars such as DMDP might explain their presence in plants. It also illustrates another very important potential application of castanospermine and derivatives as inhibitors or stimulators of processes mediated by carbohydrate-recognizing proteins such as lectins or transporters as opposed to inhibition of enzymes. Inhibition of α-D-glucosidase activity by castanospermine (**1a**) has also been demonstrated to be useful in regulating the biological effects of the stable ascorbate prodrug, 2-*O*-α-D-glucopyranosyl-L-ascorbic acid (AA-2G) [204-207], Addition of castanospermine (**1a**) to cultures of human fibroblasts and murine

spienocytes or human peripheral blood lymphocytes inhibits the AA-2G-induced synthesis of collagen and production of antibodies, respectively. This suggests that the AA-2G is hydrolyzed by a cellular α-D-glucosidase to release ascorbate, possibly after transport to the lysosomes. Perfusion studies using the guinea pig small intestine showed that AA-2G disappeared from the perfusate but that intact AA-2G was not detected in the portal vein. These observations indicated that AA-2G was hydrolyzed by brush border α-D-glucosidase activity and the released ascorbate taken up. The loss of AA-2G from the perfusate and absorption of ascorbate was completely prevented by the addition of castanospermine (**1a**), presumably through inhibition of the brush-border α-D-glucosidases [206]. These results suggest that the concentration of active L-ascorbate in humans and human cells, which like guinea pigs lack the pathway for synthesizing L-ascorbate from D-glucuronate, could be modulated by castanospermine (**1a**).

1.3.2.1.2 Lysosomal Glucosidases

Intraperitoneal injection of castanospermine (**1a**) at greater than 1 mg/g body weight for 3 days into rats leads to intralysosomal accumulation of glycogen, as in Pompe disease, the lysosomal storage disease resulting from a genetic deficiency of lysosomal α-D-glucosidase [208]. Prolonged administration of castanospermine (**1a**) at 143.6 mg/kg/day for 28 days *via* sub-cutaneous osmotic minipumps did not cause clinical signs in rats but microscopic examination showed degenerative vacuolation of hepatocytes and skeletal myocytes as in Pompe disease [160]. There was also mild vacuolation of the renal tubular and thyroid follicular epithelia. In these experiments with relatively high doses of castanospermine (**1a**), gastrointestinal problems were

avoided by removing sucrose from the diet. Although disruption of lysosomal turnover of glycogen is theoretically a hazard of any therapeutic use of castanospermine, it is probable that the doses used for therapeutic purposes will be too low to induce lysosomal storage [209]. Castanospermine (**1a**) also inhibits lysosomal β-D-glucosidase (glucocerebrosidase), the enzyme deficient in the most common lysosomal storage disease, Gaucher disease [147]. However, the K_i for human fibroblast lysosomal β-D-glucosidase is 7 mM, much higher than that for the corresponding α-D-glucosidase of 0.1 mM. Although fibroblasts in culture appear to be permeant to castanospermine (**1a**), there was no evidence of accumulation of glucocerebroside. Fibroblasts from patients with Gaucher disease type 2, the most severe form of the disease, also do not accumulate glucocerebroside. This is either due to the low turnover of glucosylceramide in fibroblasts or to diversion of undegradable glucosylceramide into biosynthetic pathways. There is a 1.5 to 2 fold increase in some other glycosphingolipids in Gaucher fibroblasts [210]. Two novel glycosphingolipids appeared in normal fibroblasts cultured in the presence of castanospermine (**1a**), supporting this explanation. However, it is also possible that they arose from inhibition of the broad specificity β-D-glucosidase, which is competitively inhibited by castanospermine (**1a**) but with a much higher K_i of 40 mM [147].

1.3.2.1.3 Processing α-D-Glucosidases

Glycoproteins play an important role in many cellular processes. These functions depend on the wide variety of asparagine *N*-linked glycans found on matural glycoproteins. This variety of structure results from the processing in the endoplasmic reticulum and Golgi apparatus of a common oligosaccharide precursor which is

transferred *en bloc* from a lipid carrier to newly synthesized proteins. The first steps in the processing of *N*-linked glycans are the removal in the endoplasmic reticulum of the outermost *a*-l→2 linked glucose by α-D-glucosidase I followed by the removal of the two *a*-1→3 linked glucose residues by α-D-glucosidase IL Both of these processing α-D-glucosidases are inhibited by castanospermine and this has been shown to prevent processing of *N*-linked glycans and to lead to the production of glycans retaining the outer α-linked glucose residues [145]. This property of castanospermine has attracted much attention because manipulation of the processing of glycoproteins could be exploited for the prevention of disease or enhancement of a beneficial process. In consequence the effects of castanospermine (**1a**) and derivatives on many cellular processes, such as intracellular transport and targeting of proteins, cell surface receptors, cell-cell recognition, cell adhesion, viral replication, the immune response, fertility and metastasis have been studied.

1.3.2.2 Antiviral Activity of Castanospermeine

Castanospermine (**1a**) was first reported to inhibit replication of the human immunodeficiency virus-1 (HIV-I) in CD4+ T cell cultures and to prevent syncitium formation at concentrations non-cytopathic to lymphocytes in 1987 [211, 212, 154]. The inhibition was reported to be synergistic with zidovudine (AZT, 3'-azido-3'-deoxythymidine) [213, 214] and other drugs [215]. A comparison of the anti-HIV activity of a series of castanospermine (**1a**) analogues revealed that 6-*O*-butanoylcastanospermine was 20-30 times more active than castanospermine (**1a**) despite having an IC_{50} 10 times greater than castanospermine (**1a**) for inhibition of α-D-glucosidase I [215, 216]. The explanation of this paradox is that

butanoylcastanospermine is taken up into cells and absorbed more rapidly into the blood stream than castanospermine (**1a**) [217]. It is subsequently rapidly hydrolyzed enzymically to castanospermine (**1a**) *i.e.* it is a prodrug. Administration of the prodrug may avoid some of the gut toxicity of the parent compound. Butanoylcastanospermine was in clinical trial as a potential anti-HIV agent. The expression of the integrin LFA-I (CD 18/CD Ua), which may decrease cell adhesion of uninfected mononuclear leukocytes [218] is also decreased by butanoylcastanospermine and this may play a role in the prevention of transfer of HIV-1 from cell to cell [158]. Subsequently, a number of analogs of castanospermine (**1a**) were synthesized and tested for their inhibition of α-D-glucosidase I *in vitro* and in cells [219]. Although the analogs were weaker inhibitors against the purified enzyme *in vitro,* those with lipophilic side chains were more effective in the cells. Substitution of oxygen for methylene groups in the alkyl chains of *N*-decyldeoxynojirimycin was found to decrease its detergent properties without affecting the intracellular blocking of glycoprotein processing [220]. Such modification may also be applicable to castanospermine (**1a**). The precise mechanism by which α-D-glucosidase inhibitors decrease HIV-infectivity is not known but experiments with the closely related *N*-butyldeoxynojirimycin show that it impairs viral entry at a post-CD4 binding step [221]. The prodrug, butanoylcastanospermine, may have several other important applications. Oral treatment of mice infected with herpes simplex virus-1 with 6-*O*-butanoylcastanospermine decreased infection in the brain and delayed development of lesions [222]. It also blocked growth of herpes simplex virus-2 [160]. The basis of the activity of castanospermine (**1a**) against herpes simplex virus is probably blocking of the association of herpes simplex viral glycoproteins with calnexin [223].

1.3.2.3 Anticancer Activity of Castanospermine

Both catabolic and processing glycosidases are involved in the transformation of normal cells to cancer cells and in tumor cell invasion and migration. Many tumor cells display aberrant glycosylation due to an altered expression of glycosyltransferases [224] and it has been known for a long time that the levels of glycosidases are elevated in the sera of many patients with different tumors [225]. Secreted glycosidases may be involved in the degradation of the extracellular matrix in tumor cell invasion [226]. The lysosomal system is extremely active in cancer cells presumably reflecting the enhanced turnover of glycoproteins and other molecules. Castanospermine (**1a**) and other glycosidase inhibitors are being investigated as potential anti-cancer agents [227, 228]. Castanospermine (**1a**) has been shown to affect many of the properties of tumor cells *in vitro* and *in vivo* [229-232]. Increased formation of new capillaries, angiogenesis, is a feature of many pathological processes including tumor growth. Castanospermine (**1a**) was found to inhibit tumor growth and angiogenesis in nude mice infected with EHSBAM tumor cells which form highly vascularized tumors [168]. Altered glycoproteins were found on endothelial cells, which had a decreased ability to migrate and invade the basement membrane. These experiments suggest that specific cell surface oligosaccharides are involved in angiogenesis and that inhibition of their formation by castanospermine (**1a**) may be a way of preventing tumor growth. The adhesion of human myeloma cells to endothelial cells [233] is enhanced by castanospermine (**1a**) whereas the interaction of integrins on carcinoma cells with fibronectin was decreased [234]. Castanospermine (**1a**) also impairs the transformation of chicken embryo fibroblasts by the virus, env-sea, by blocking transport to the cell surface of proteins encoded by the env-sea oncogene

[235]. Thus the consequences of inhibition of processing α-D-glucosidase by castanospermine (**1a**) in cancer pathology are diverse.

1.3.2.4 Other Cellular Processes

The decrease in the appearance on the cell surface of specific carbohydrate structures or glycoproteins by inhibition of processing α-D-glucosidase by castanospermine (**1a**) is being investigated as a means of modulating other important cellular processes. The anti-inflammatory properties of castanospermine (**1a**) in an adjuvantinduced rat model of arthritis have been attributed to prevention of the expression of leukocyte cell surface-bound enzymes or of adhesion molecules involved in the capture and retention of the leukocytes in the inflamed tissue [236]. Both of these changes would affect the passage of the leukocytes through the sub-endothelial basement membrane. Subsequent work showed that although castanospermine (**1a**) selectively inhibited the phorbol myristate-induced heparanase and sulfatase activity of endothelial cells, it did not inhibit the constitutive expression of enzymes for degradation of the extracellular matrix by non-stimulated cells [172].

The alteration in the expression of cell surface glycoproteins induced by castanospermine may be useful in modulating the immune response. The reduction in expression of adhesion molecules can prolong heart allograft survival in rats [174] and pancreatic duodenal allograft survival is prolonged in an experimental form of treatment for diabetes in rats [237]. Castanospermine (**1a**) can act synergistically with other drugs in prolonging allografts [175, 176].

Other cellular processes affected by the castanospermine-induced alteration in the expression of cell surface glycoproteins include interleukin-4 induced macrophage

fusion and the formation of giant cells involving the mannose receptor [238], fusion of myoblasts to form multinucleated myotubes [239], oligodendrocyte differentiation in cell culture [240, 241], neurite outgrowth *in vivo* during development and regeneration [242] and gap junction formation [243].

Although glycosidases are very abundant in the male reproductive tract, and have a characteristic distribution along the epididymis, their function is not fully understood. Continuous administration of castanospermine (**1a**) to rats suppressed the epididymal α-D-glucosidase within 2 days but only decreased fertility transiently [244]. It was concluded that the epididymal α-D-glucosidase does not play a crucial role in the development of sperm fertility but may be involved in preparation of spermatozoa for storage.

Castanospermine (**1a**) and its analogs have become standard tools for investigating properties of individual glycoproteins and cellular processes dependent on glycosylation. The response of an animal cell to castanospermine (**1a**) will depend on its function, physiological state, tissue environment and the concentration of castanospermine (**1a**) to which it is exposed. As most cells contain several susceptible glucosidases with different sub-cellular locations, pH-optima and inhibition constants, the effect may be complicated. However the extracellular and resultant intracellular concentration of castanospermine (**1a**) required causing inhibition of the processing glucosidases appears to be much lower than that required to inhibit the lysosomal enzymes. Therefore, therapeutic applications exploiting inhibition of the processing or digestive glucosidases may not be complicated by induced storage of glycogen.

1.3.3 Syntheses of Castanospermine and Its Stereoisomers

The first isolation of castanospermine (**1a**) from the seeds of *C. australe* was revealed in 1981 by Hohenschutz *et al.* Three years later, in 1984, Bernotas and Ganem reported the earliest total synthesis of castanospermine (**1a**) [245] by utilizing the D-glucose derivative, 2,3,4-tri-*O*-benzyl-D-glucopyranose (7) as the starting material (Scheme 1). A key step was the formation of the piperidine ring by cyclization of the epoxide **11** (R = H) by the deprotection of **11** (R = $COCF_3$) with $NaBH_4$/EtOH. This reaction gave a 55:45 mixture of the azepine **13** and the desired piperidine **14**.

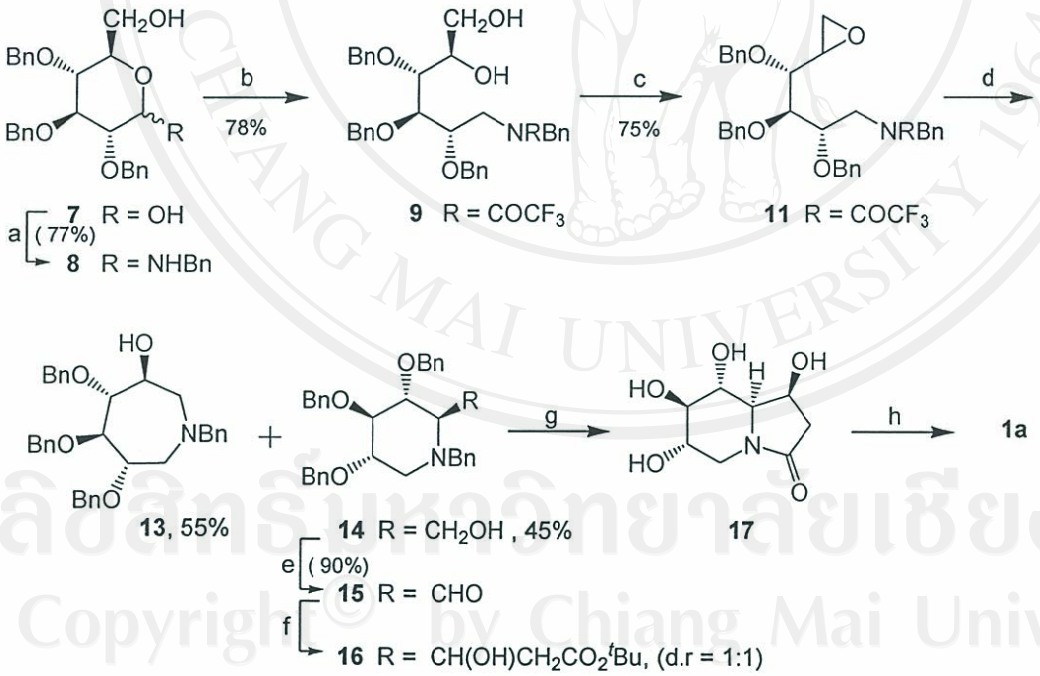

Scheme 1 *Reagents* (a) Benzylamine, $CHCl_3$, rt; (b) i. $LiAlH_4$, THF, reflux, 5 h, ii. TFAA, rt; (c) i. *t*-$BuMe_2SiCl$-imidazole, ii. MsCl, pyridine, 5°C, iii. Bu_4NF-THF, CH_3ONa-CH_3OH; (d) $NaBH_4$, EtOH, 40 °C, quant. yield; (e) DMSO, $(COCl)_2$, DCM, Et_3N, -78 °C, 1 h; (f) Lithio *t*-butyl acetate, THF, -40 °C; (g) i. hydrogenolysis, ii. TFA-H_2O, 60 °C, 3h; (h) DIBAL-H, THF, -78 °C.

In 1985, Hashimoto *et al.* [246] described a total synthesis of castanospermine (**1a**) from D-mannose by using double cyclization of **18c** as the key step. The first of key step was the piperidine ring closure (as depicted in **18c** by arrow *a*) and followed by the pyrrolidone ring formation (arrow *b*) to give **19** as showed in Scheme 2. The requisite intermediate **18a** was derived from the starting compound diol **20a** (Scheme 3), which was prepared from D-mannose. Since the isolation of the desired product **18a** from its diastereoisomer, **29a**, at this stage was found to be rather difficult, the mixture was converted to **18c** and **29c** then refluxed in methoxyethanol to afford as expected the indolizidinones **19** and **30**. Silica gel chromatography separated **19** and **30** in 31% and 30 % yield, respectively (Scheme 3). The same procedure was applied to **29a** to give (+)-1-epicastanospermine (**1c**) as the final product.

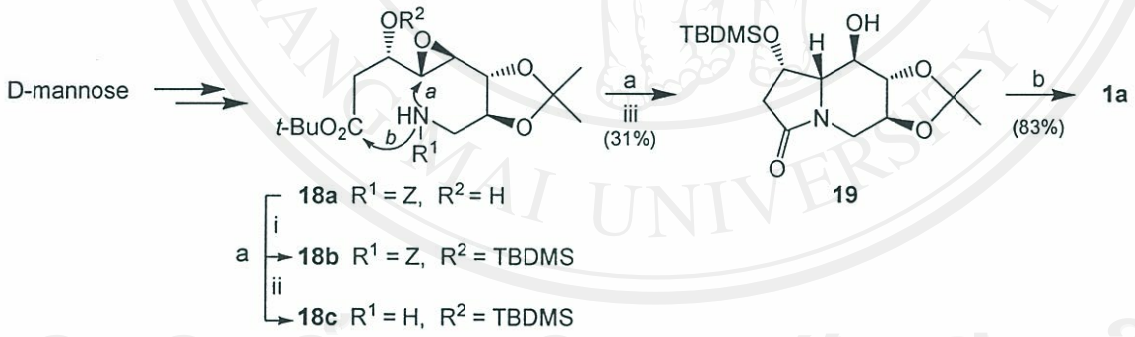

Scheme 2 *Reagents* (a) i. TBDMSCl, imidazole, DMF, 80 °C, ii. Pd-C in EtOH, iii. amethoxyethanol, reflux; (b) i. borane-THF, THF, reflux, ii. 6 N HCl, THF, reflux.

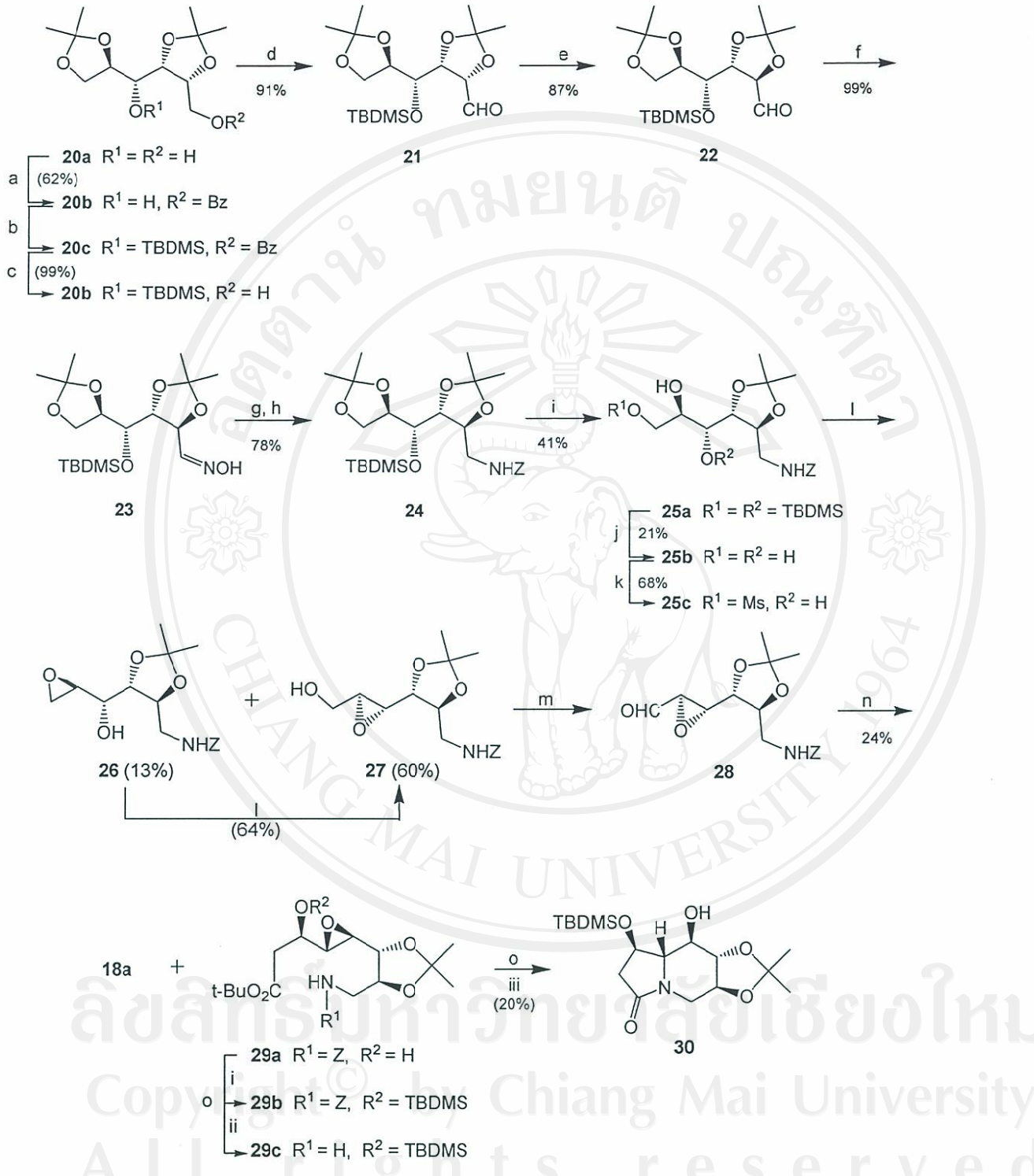

Scheme 3 *Reagents* (a) BzCl, pyridine, rt; (b) TBDMSCl, imidazole, DMF, 80 °C, (c) 1 N NaOH, MeOH, rt; (d) DMSO, DCC, TFA, pyridine, benzene, rt; (e) K_2CO_3 (3 equiv), MeOH, rt; (f) $H_2NOH{\cdot}HCl$, $NaHCO_3$, EtOH-H_2O, 60 °C; (g) $LiAlH_4$, THF, rt, (h) ZCl, THF-H_2O, 0 °C; (i) TsOH (0.1 eqiuv.), MeOH-H_2O 9:1, 15 °C; (j) *n*-Bu_4NF, THF, 0 °C; (k) MsCl, pyridine, 5 °C; (l) MeONa (1.4 equiv.), MeOH, 20 °C; (m) $CrO_3{\cdot}2$ pyridine, DCM, 5 °C; (n) *t*-

butyl lithioacetate, THF, 0 °C; (o) i. TBDMSCl, imidazole, DMF, 80 °C, ii. Pd-C in EtOH, iii. methoxyethanol, reflux.

The synthesis of the castanospermine **1a** which relied on a general method for heteroatom-selective chelation during Sakurai allylation of aza-gluco aldehydes (e.g. **15**), was revealed by Ganem *et al.* in 1987 as shown in Scheme 4 [247].

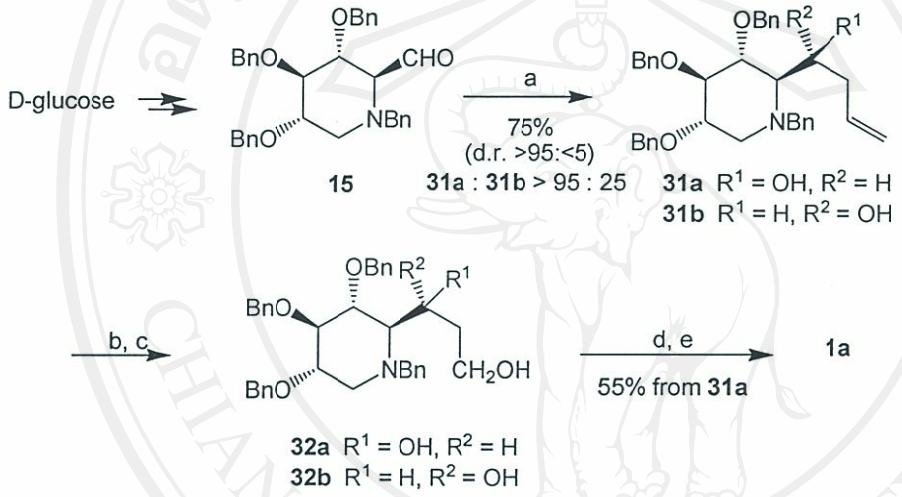

Scheme 4 *Reagents* (a) allyltrimethylsilane (3.6 equiv), $TiCl_4$ (2.4 equiv), DCM, - 85°C, 15 h; (b) O_3, DCM, -78 °C; (c) $NaBH_4$, ethanol; (d) MsCl, Et_3N, DCM; (e) H_2, Pd/C.

The synthesis of **1a** from 7-oxabicyclo[2.2.1]hept-5-en-2-one benzyl acetal was reported in 1989 by Vogel and co-worker [248] (Scheme 5). They began the synthesis by bromination of the dibenzyl acetal **33** which gave the protected bromohydrine **36**. The results could be interpreted in terms of formation of intermediates **34** and **35** that lead to the stereoselective migration of the *endo* BnO group of the acetal. Oxidation of **36** with mCPBA furnished lactone **37**. Treatment of **37** with MeOH and $SOCl_2$ gave the methylfuranoside **38** and its anomer [249].

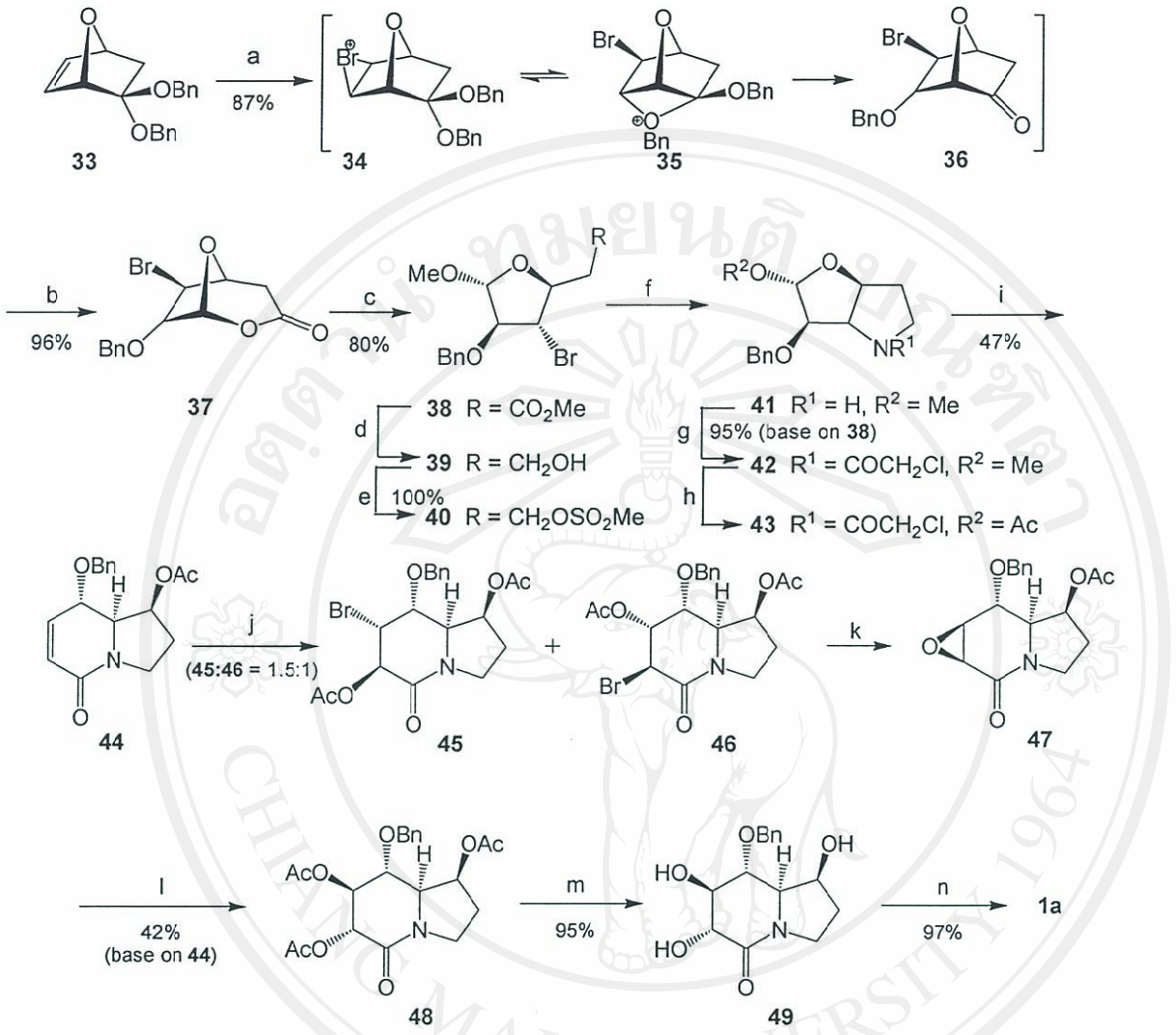

Scheme 5 *Reagents* (a) Br_2, DCM, -80°C; (b) mCPBA, $NaHCO_3$, DCM, 5-20°C; (c) MeOH, $SOCl_2$, 20°C, 24 h; (d) DIBAL-H, THF, -50 to -20°C; (e) CH_3SO_3Cl, Et_3N, DCM, 0°C; (f) 12% NH_3, EtOH/H_2O 1:1, 70°C, 5 h; (g) $ClCH_2COCl$, pyridine, DCM, -5-8°C; (h) Ac_2O, H_2SO_4 conc., 5°C, 2 h; (i) i. $(EtO)_3P$, 130°C, 7 h, ii. K_2CO_3, EtOH, 20°C, 12 h, iii. Ac_2O, pyridine, 4-dimethyaminopyridine, 20°C, 48 h; (j) Br_2, 1:2 AcOH:Ac_2O, AgOAc, 9°C; (k) i. $SOCl_2$, MeOH, 20°C, 17 h, ii. 2-*t*-butylimino-2-diethylamino-1,3-dimethylperhydro-1,3,2-diazphosphorine on polystyrene, CH_3CN, 20°C, 30 min; (l) i. H_2O, 100°C, 4.5 h, ii. Ac_2O, pyridine and 4-dimethyaminopyridine, 20°C, 48 h; (m) $BH_3{\cdot}Me_2S$, THF, 20°C, 15 h; (n) H_2, 10% Pd-C, 5:1 THF-H_2O, 24 h.

Reduction of **38** afforded **39** which was esterified to give the mesylate **40** followed by heating with ammonia in ethanol and water afforded the cyclized product,

41. The crude amine **41** was treated with $ClCH_2COCl$/pyridine to give amide **42** then treated with Ac_2O in concentrated sulfuric acid to afford the acetate **43** which was converted into the lactame **44** through an intramolecular Horner-Emmons condensation on heating with $(EtO)_3P$ followed by treatment with K_2CO_3 in EtOH then acetylation. Bromination of **44** gave a 1.5:1 mixture of **45** and **46** which was converted into the epoxide **47**. After oxirane hydrolysis, the resulting product was acetylted to give triacetate **48**. Reduction of **48** furnished **49** which was debenzylated to give **1a** as the final product.

Anzeveno *et al.* reported the highly stereoselective synthesis of **1a** from 1,2-*O*-isopropylidine-α-D-glucofuranurono-6,3-lactone (**50**) as shown in Scheme 6 [250]. *N*-Boc-amino-desoxy-glucuronolactone **51**, was obtained from the starting glucuronolactone, **50**, in three steps. Treatment of **51** with ethyl acetate and LDA gave **52** as a single epimer **52**. Reduction of **52** with sodium borohydride gave rise to product mixtures containing both **53a** and **53b**, with **53b** as the predominant component. This high diastereoseclectivity may be due to some coordination of the reducing agent with the oxygen functions of keto-ester intermediate **A** (in equilibrium with **52**) as depicted in Figure 12A. Conversely, catalytic hydrogenation of **52** over Pt in EtOAc at 45-50 psi gave reproducible 7:2 mixtures of **53a** and **53b**. This preference could be rationalized by assuming that the favored reaction conformer of **52** is that pictured in Figure 12B and that hydrogen transfer takes place for the most part, from the direction opposite to the sterically demand of *t*-butyl carbamate group. Boc-amino-diol, **53a**, could be deprotected by treatment with formic acid. The result amino ester cyclized during purification over DOWEX 1×2 basic ion exchange resin to afford

lactam **54**. LAH reduction of **54** gave a yield of furano-pyrrolidine **55**, which upon treatment with 90% TFA followed by catalytic hydrogenation over Pt on C gave the desired product, **1a**, in 61 % yield (from **55**).

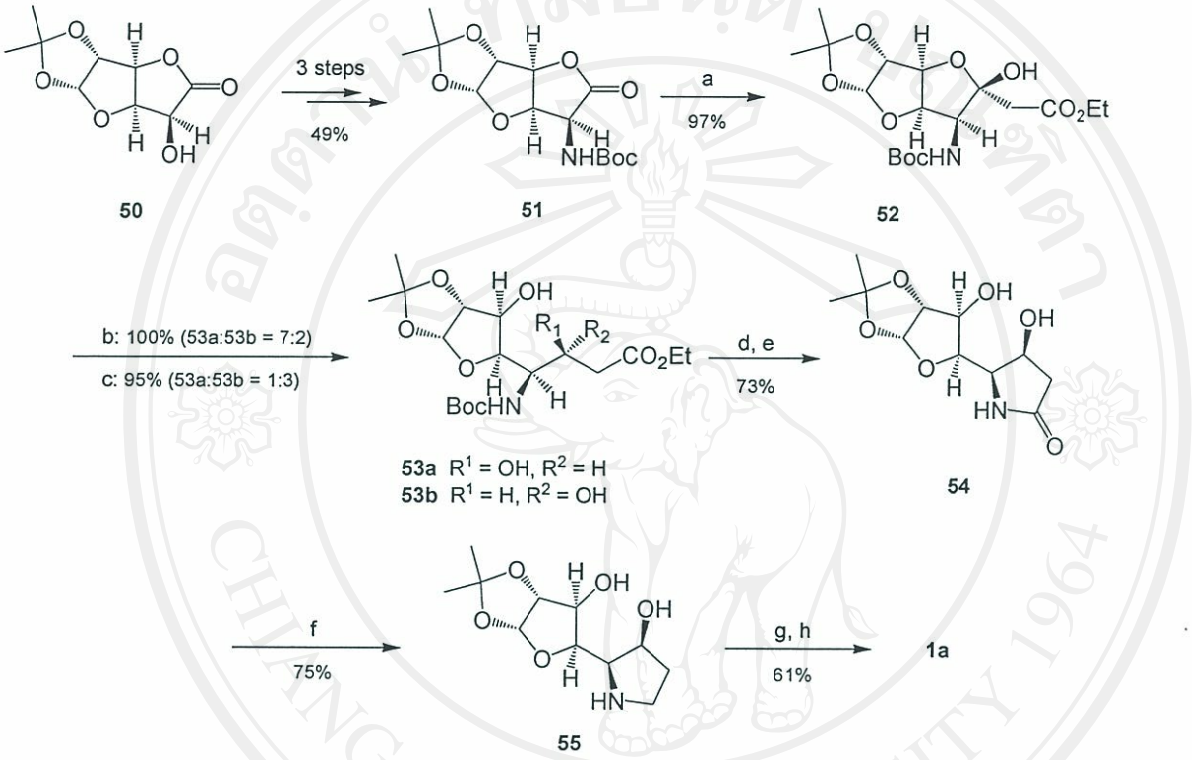

Scheme 6 *Reagents* (a) EtOAc (3 equiv), LDA (3 equiv), THF, -78°C, 2.5 h; (b) H_2 (45-50 psi), PtO_2, EtOAc, 20 h; (c) $NaBH_4$ (0.5 equiv), EtOH, 0°C, 1 h; (d) HCO_2H (98%), DCM, 0-5°C (2 h) then 25°C (6 h); (e) Dowex 1×2 (OH^-) resin, H_2O; (f) LAH (5 equiv), THF, reflux, 20 h; (g) TFA (90%), 25°C, 20 h; (h) H_2 (50 psi), 5% Pt/C, H_2O, 20h (61% , two steps).

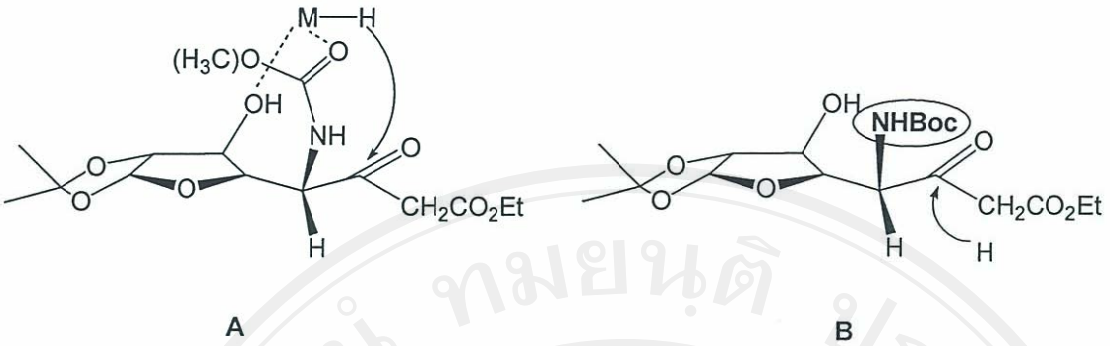

Figure 12 A) Coordination of reducing agent (M-H) with intermediate **A**. B) Favored direction of hydrogen transfer due to steric group (NHBoc) in **B**.

A chemoenzymatic synthesis of **1a** was proposed by Sih *et al*. They utilized the yeast *Dipodascus sp.* in the Vogel's medium as a catalyst for the transformation of **56** to the starting material **57** in yield of 80% and >99% ee (Scheme 7). Optically pure **58** was conversed from **57** then transformed into diester, **59**, by treatment with TFA followed by treatment with triethylamine and methyl acrylate. Acryloin condensation of **58** in the presence of an excess of TMSCl afforded the bistrimethylsilyoxy derivative, **60**. Hydrolysis of **60** gave a mixture of **61** and **62**. Apparently, under acidic conditions the hydroxyl group at C-8 partially epimerized. The inversion of the C-8 center was more completely achieved by stirring **61** with DBU to furnish a mixture of **63** and **62** in approximately a 1:1 ratio. In the presence of an excess of DBU, the compound **60** was also converted to a mixture of **63** and **62**. The mixture was quantitatively converted into **64**. Hydroboration of **64** followed by subsequent oxidation of the borane complex gave a mixture of **65** (15%), **66** (24%) and **67** (32%). Desilylation of **66** afforded **1a** in an excellent yield [251] (Scheme 8). The same method when applied to **65** and **67** gave 1,8-diepiswainsonine and 6,7-diepicastanospermine **1g**, respectively.

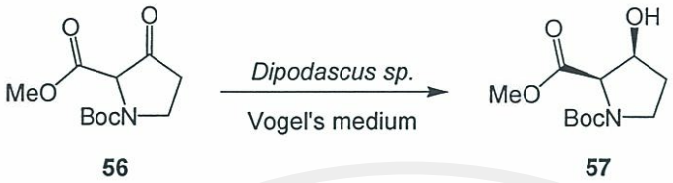

56 57

Scheme 7

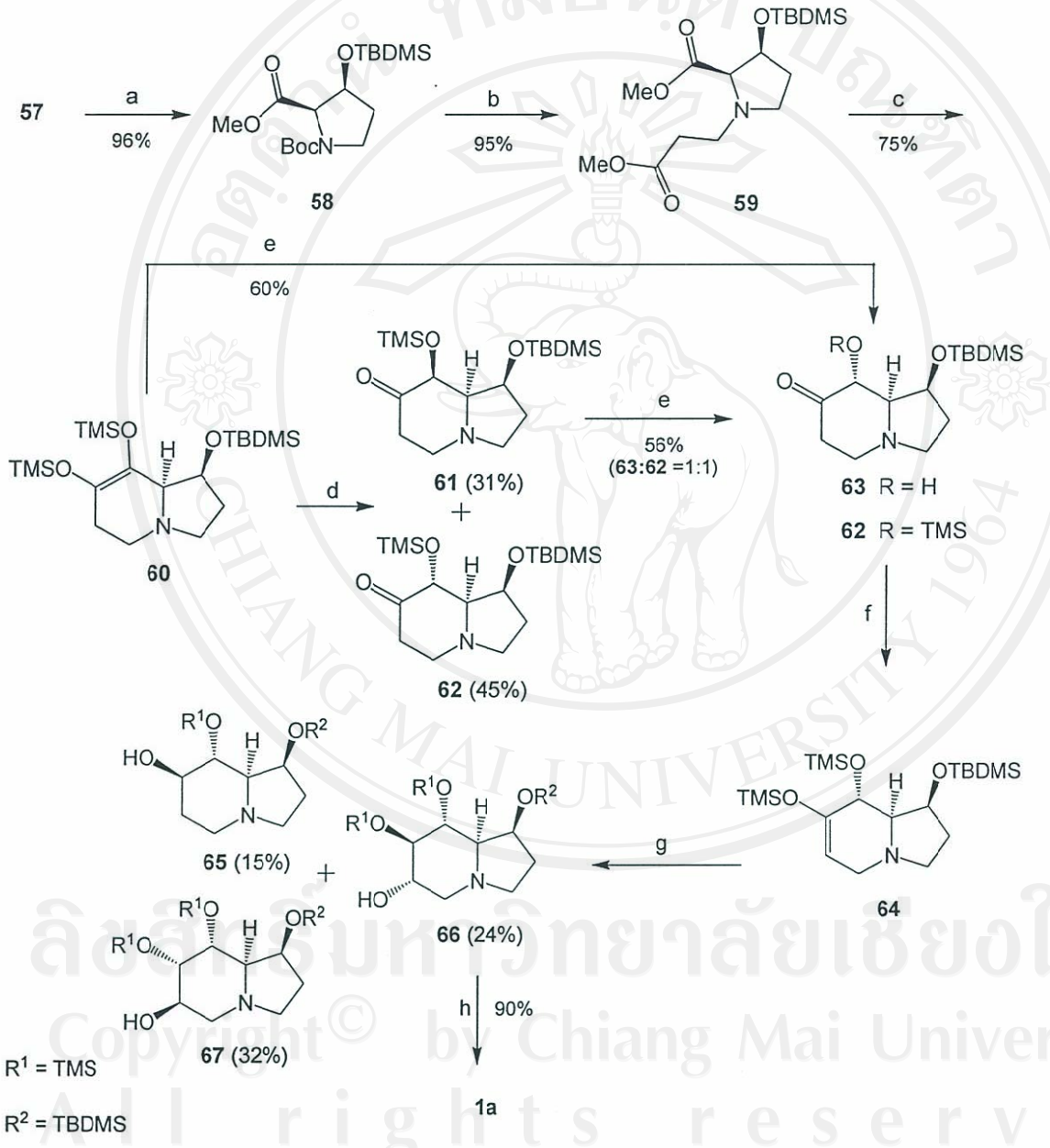

Scheme 8 *Reagents* (a) TBDMSCl, imidazole, DCM, 24°C, 2 h; (b) i. 20% TFA, DCM, ii. Et_3N (3 equiv), methyl acrylate (1.5 equiv), EtOH; (c) Na (4.2 equiv), TMSCl (5 equiv), toluene, reflux; (d) AcOH, NaOAc (10%), 24°C, 2 h; (e) DBU, DCM, 24 °C, 48 h; (f) TMSCl,

$LiN(TMS)_2$, -78°C, THF; (g) i. BH_3, Me_2S (2 equiv), THF, -78°C to 25°C, 12 h ii. Me_3NO (10 equiv), toluene, reflux; (h) *n*-Bu_4NF, THF, 0°C to 25°C, 2 hr.

Miller and Chamberlin [252] proposed the enatioselective hydroxylactam strategy for synthesis of **1a**. Preparation of the requisite hydroxyl lactam **69** began with the known 6-*O*-acetyl-2,3,4-tri-*O*-benzyl-D-glucono-1,5-lactone, **68**, which was treated with 2-[3-aminopropyllidine]-1,3-dithiane followed by lead tetraacetate oxidation, to afford the expected hydroxylactam **69** as a mixture of epimers (Scheme 9). Without separation, this mixture was cyclized to indolizidine ring system by adding methanesulfonyl chloride and triethylamine in dichloromethane, give a good yield of ring juncture epimers **70** and **71** in approximately a 1:1 ratio. After separation, the simple ketene dithioacetal group of **70** was oxidative cleaved via ozonolysis to give the unstable ketone, **72**, followed by reduction to alcohol **73** with L-selectride gave the desired epimer **73** in 39% overall yield. Treatment of **73** with borane-dimethyl sulfide complex followed by the debenzylation step gave **1a** in 82% yield.

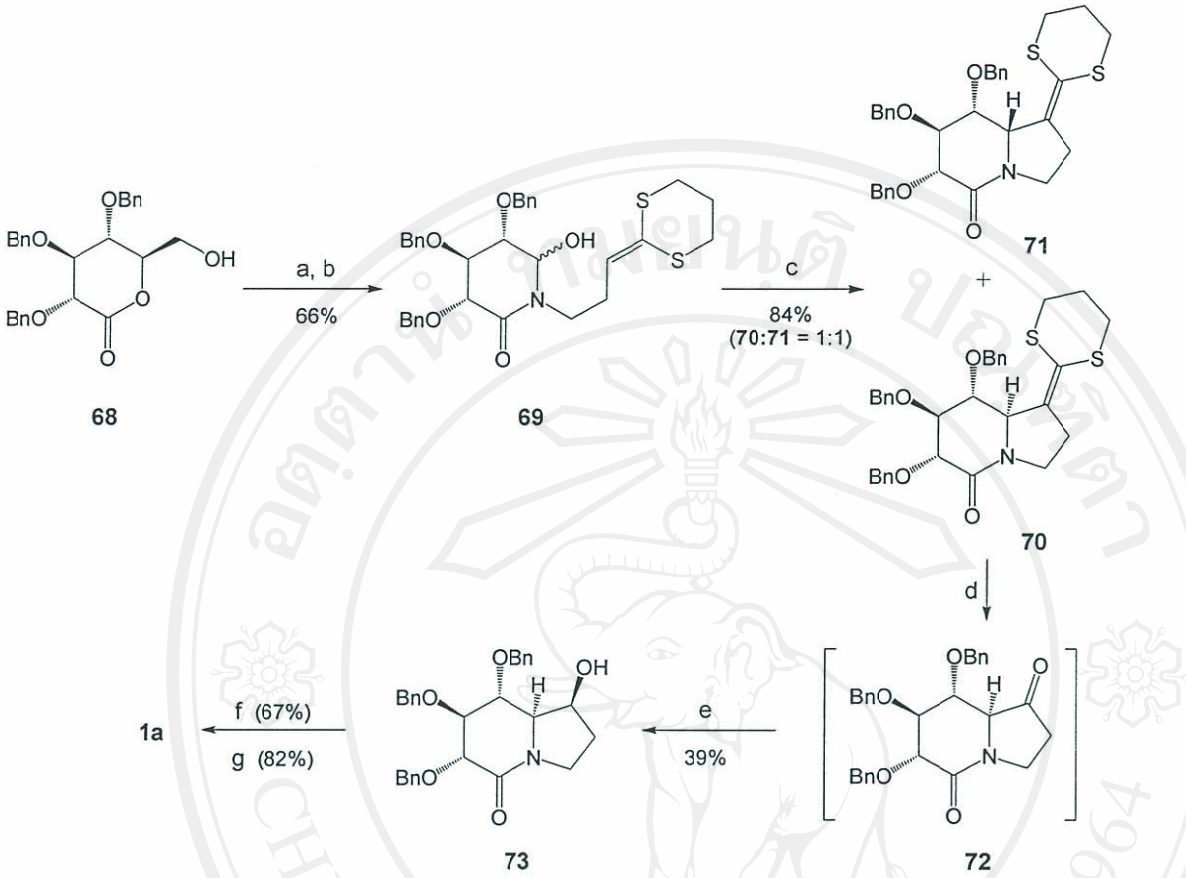

Scheme 9 *Reagents* (a) 2-(3-aminopropylidine)-1,3-dithiane, MeOH; (b) $Pb(OAc)_4$, CH_3CN, then AcOH; (c) Et_3N, MsCl, DCM; (d) O_2, CCl_4/MeOH; (e) L-Selectride,THF; (f) BH_3/DMS, THF; (g) H_2, 10% Pd/C, MeOH/HCl.

In 1990, the stereoselective synthesis of castanospermine **1a**, from a non-carbohydrate precursor was revealed by Ina and Kibayashi [253]. Their synthesis began with the epoxide **75** which was conveniently obtained from **74** by Sharpless epoxidation. Regiospecific cleavage of the oxirane ring was achieved by exposure of **75** to $Et_2AlN(CH_2Ph)_2$ to give diol alcohol **76**. Two hydroxyl groups of **76** were sequentially protected by treatment with one equivalent of acetyl chloride followed by methoxymethyl chroride, affording **77**. After deacetylation by treatment with $LiAlH_4$, the resulting alcohol was converted to the aldehyde **78** by Swern oxidation. The

aldehyde **78** was allowed to reacted with the $LiN(SiMe_3)_2$ and ethyl acetate to provide an inseparable 9:1 ratio of the esters **79** and **80**. The formation of the major epimer **79** in this aldol addition could be explained by the chlelate model A with a chair-chair transition state arrangement, in which the enolate added to the *si* face of the aldehyde carbonyl (Figure 13) The alternative chair arrangement B leading to the ester **80**, however, displayed unfavorable nonbonded interactions between the R group (at C-3 position in **79**) and the enolate carbon. The mixture of **79** and **80** was subjected to $LiAlH_4$ reduction followed by protection with *t*-butyldimethylsilyl chloride to give a separable mixture of the major **81** and minor **82** components. Undesired major isomer **81** was converted to the requisite epimer **82** by Mitsunobu displacement with acetic acid followed by deacetylation of the resulting acetate **83** with $LiAlH_4$. Silyl ether deprotection and subsequent tosylation of **83** gave the ditosylate **85**. Debenzylation of **85** was performed via the hydrogenolysis over palladium hydroxide in methanol. Triethylamine was then added to the resulting primary amine which was then heated to furnish the cyclized product **86**. Removal of the protecting groups in **86** with acid in methanol at reflux provided **1a** in a good yield (Scheme 10). A full reportion on this work was republished 1993, by the same researchers.

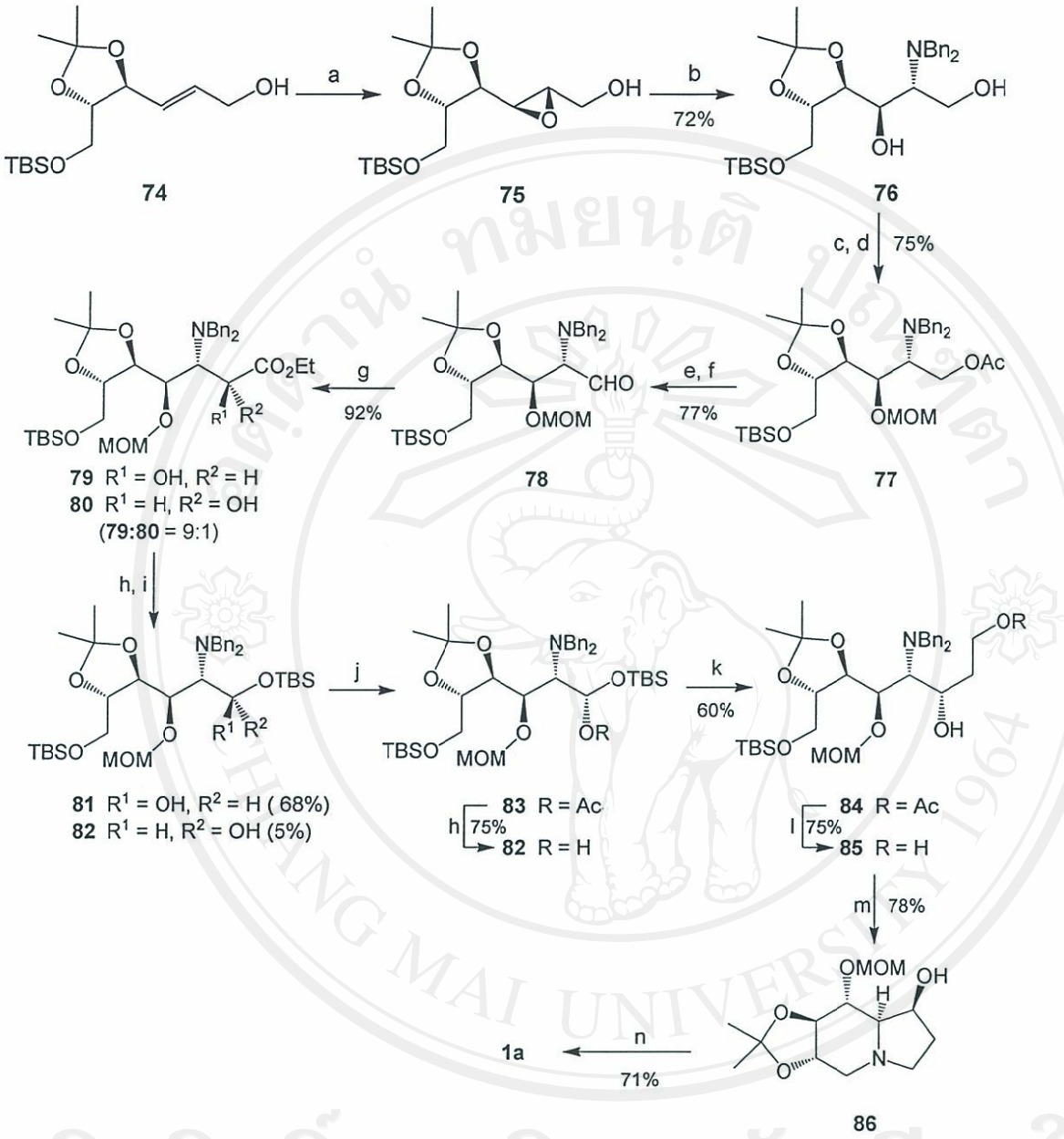

Scheme 10 *Reagents* (a) Sharpless epoxidation, (b) $Et_2AlN(CH_2Ph)_2$, DCM, rt; (c) AcCl (1 equiv), Et_3N, DCM, 0°C; (d) CH_3OCH_2Cl, *i*-Pr_2NEt, $CHCl_3$, reflux; (e) $LiAlH_4$, Et_2O, rt; (f) DMSO, $(COCl)_2$, Et_3N, DCM, -78°C to rt; (g) AcOEt, $LiN(SiMe_3)_2$, THF, -78°C; (h) $LiAlH_4$, Et_2O, rt; (i) *t*-$Bu(Me)_2SiCl$, imidazole, DMF, rt; (j) AcOH, Ph_3P, $(EtOCON=)_2$, C_6H_6, reflux; (k) *n*-Bu_4NF, THF, rt; (l) TsCl (2 equiv), pyridine, rt; (m) H_2, $Pd(OH)_2$, MeOH, then Et_3N, MeOH, reflux; (n) HCl, MeOH, reflux.

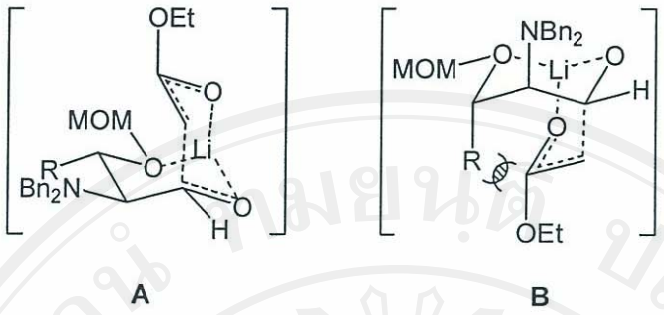

Figure 13 The model of the favor (**A**) and disfavor (**B**) chelating of aldehyde **78** and AcOEt in the presence of Li-complex.

To prepare castanospermine **1a**, Gerspacher and Rapoport have utilized 3-pyrrolidinone **(88)** as the starting material, which was obtained from glucono-δ-lactone (**87**) in more than 8 steps [254]. The synthesis begun by treatment of 3-pyrrolidinone **(88)** with an excess acetic anhydride in pyridine to selectively acylate the primary hydroxyl and form the monoacetate **89**. From monoacetate **89**, the trifate **90** was afforded by reaction with triflic anhydride. The unpurified resulting product was then subjected to a solution of *t*-butylammonium acetate followed by treatment with Ac_2O/pyridine/DMP to obtain diacetate **91**. The keto group in **91** was reduced by treatment with $NaBH_4$ and then deacetylation of the resulting product gave the triol **93**. Tosylation of the primary hydroxyl of **93** was achieved, followed by removal of the phenylfluorenyl group by hydogenolysis to afford cyclized product, **95**. The isopropylidine group of indolizine **95** was then cleaved by treatment with TFA to give the desired product **1a** (Scheme 11).

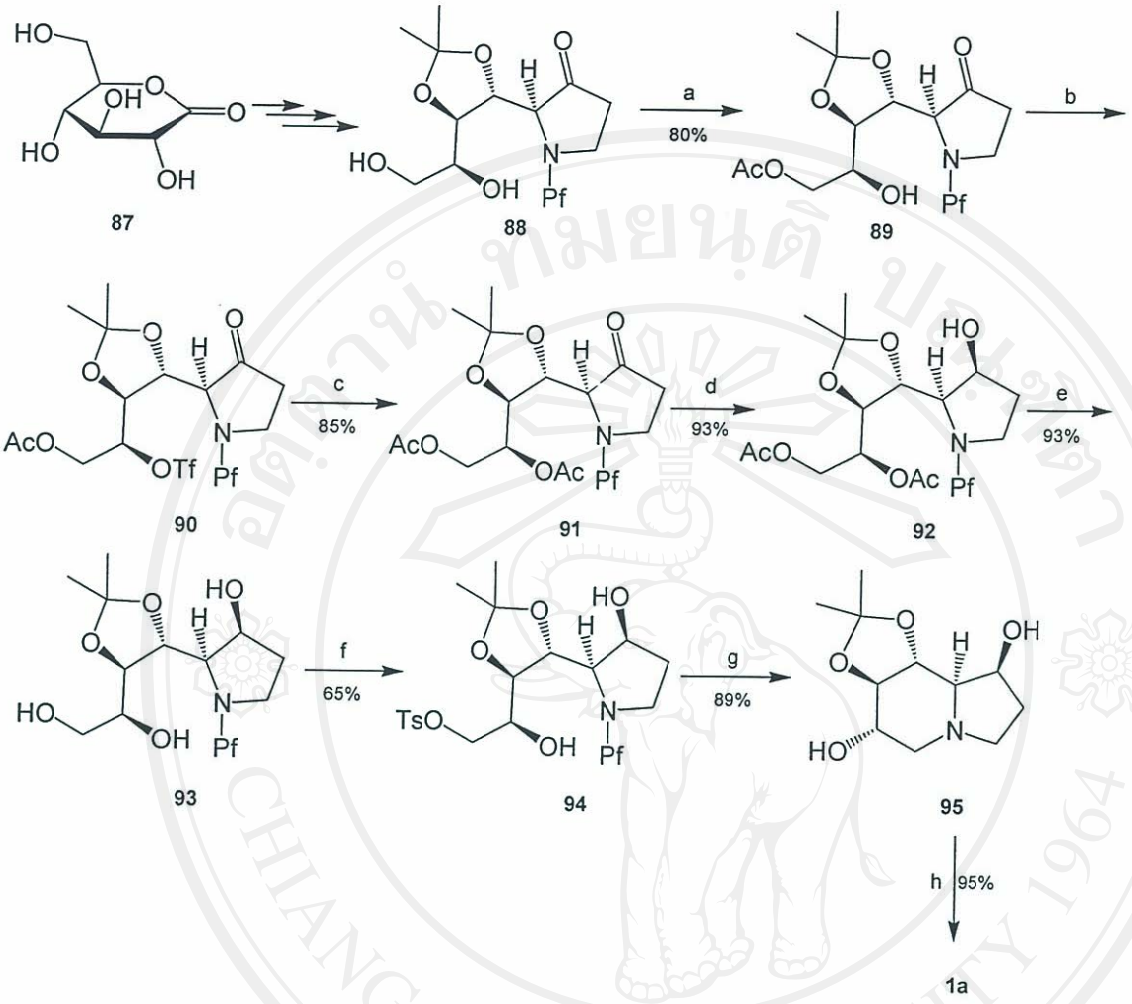

Scheme 11 *Reagents* (a) Ac_2O, pyridine, 0°C, 20h; (b) Tf_2O, pyridine, DCM, -15°C, 20 min; (c) i. tetrabutylammonium acetate, CH_3CN, 40°C, 50 min, ii. Ac_2O, pyridine, DMAP, rt, 3 h; (d) $NaBH_4$, absolute EtOH, 0°C, 90 min; (e) K_2CO_3, MeOH, 0°C, 1 h; (f) TsCl, DMAP, DCM, 0°C, 1 h; (g) Pd/C, NaOAc, MeOH, rt, 20 h then reflux 10 min.; (h) TFA/water/dioxane (1:1:1.3), rt, 20 h.

Cha and co-worker [257] reported another synthesis of castanospermine **1a** by utilizing Sharpless epoxidation as the key step. Their pathway started with the conversion of the lactol **96** by an iterative Wittig protocol and subsequent tosylation into the diene **97**. Desilylation and asymmetric Sharpless epoxidation afforded epoxide **98** as a single isomer which upon azide displacement of the tosylate gave **99**.

Asymmetric dihydroxylation of the remaining double bond with OsO_4 in the presence of chiral ligand [$(DHQ)_2$-PHAL], afforded the pair of diols **100** and **101** in a ratio of 10:1 while used of the alternative ligand [$(DHQD)_2$-PHAL] generated a ratio of 1:20. Reduction of the azide moiety in **100** led to the indolizidine lactam **101**, (isolated as the tetraacetate **103**) Reduction of the lactam and deacetylation then afforded castanospermine **1a**. The same procedure applied to **101** gave 6,7-diepicastanospermine **1g** (Scheme 12).

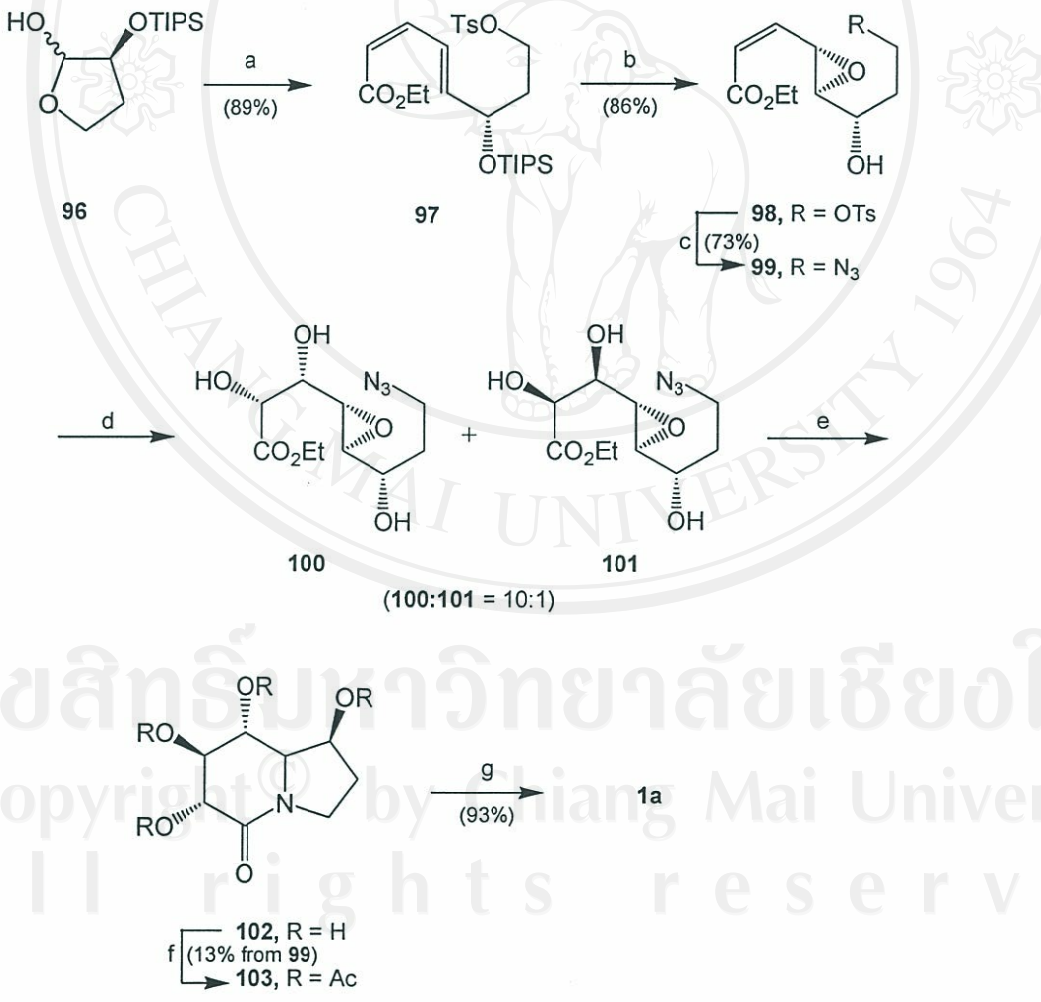

Scheme 12 *Reagents* (a) (4*S*)-4-(triisopropylsiloxy)-6-[(*p*-toluenesulfonyloxy]-(*E*)-2-hexenal, (carbethoxymethylene)triphenylphosphorane, 50°C, 1.5 h; (b) $Ti(O^iPr)_4$, (+)DIPT, *t*-BuOOH, TBAF, DCM, -23°C, overnight; (c) NaN_3, DMF, rt, 14 h; (d) $K_3[F(CN)_6]$, K_2CO_3,

$(DHQ)_2$-PHAL, K_2OsO_4, water/*t*-BuOH, rt, 12 h; (e) 10% Pd/C, EtOH, rt, 6 h; (f) Ac_2O, pyridine, rt, 20 h; (g) i. BH_3-Me_2S, THF, rt, 3 days, ii. 20% NH_3, rt, 12 h.

An elegant triple reductive amination approach to castanospermine **1a** has been described by Zhao and Mootoo in 1996 and 2001 [258, 259]. They began with the allylation of the readily available D-glucose derivative **104** to generate a 9:1 ratio of stereoisomers, and then *O*-benzylation of the major isomer afforded **105**. A cleaver manipulation of this material using iodonuim dicollidine perchlorate then reduction with zinc produced the olefin **106** with the C-5 hydroxy group selectively exposed for oxidation. Swern oxidation of **106** followed by ozonolysis of the olefin and hydrolysis of the dimethyl acetal moiety produced the dialdosulose derivative **108** as a mixture of lactol isomer. Triple reductive amination of this material successfully afforded tetra-*O*-benzylcastanospermine **110** (53% yield) which provided castanospermine **1a** after transfer hydrogenolysis in an overall yield of 22% (from starting compound **104**) (Scheme 13)

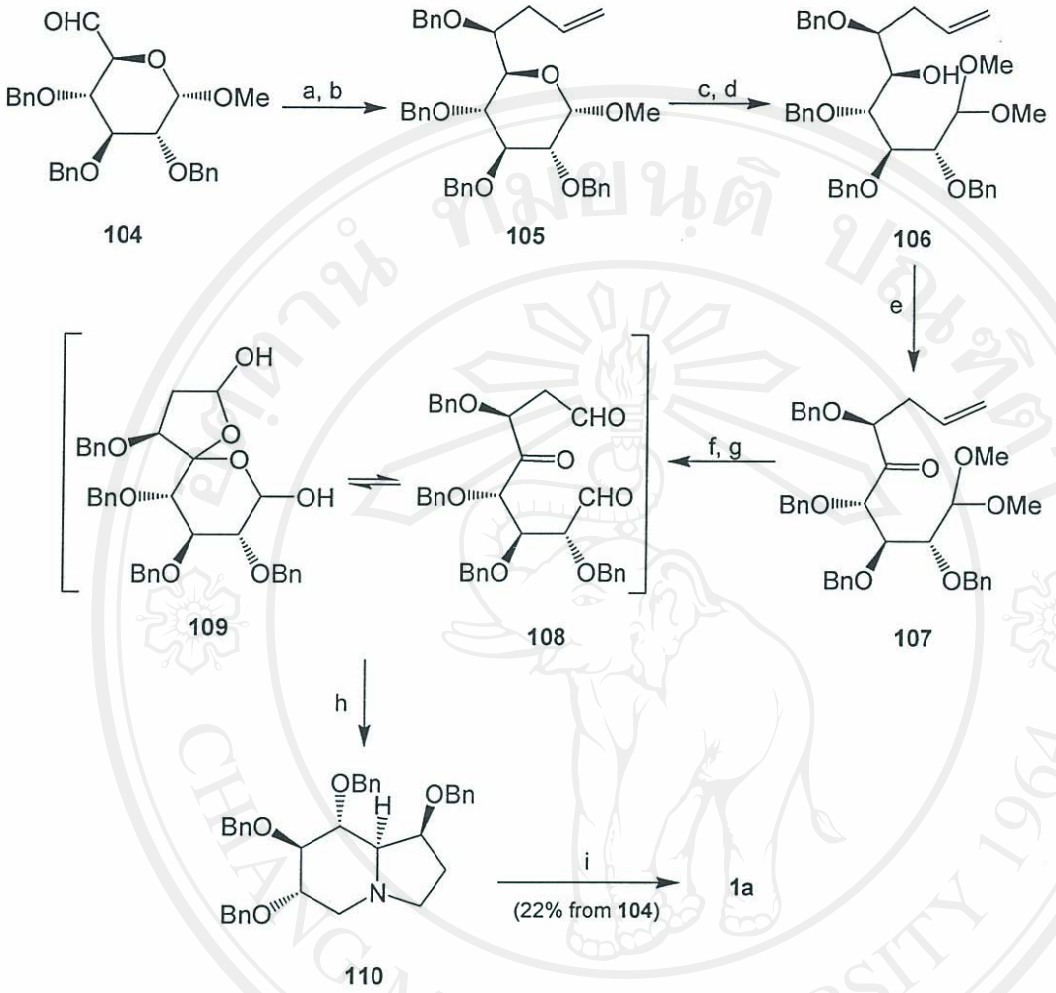

Scheme 13 *Reagents* (a) allylbromide, Sn, CH_3CN/H_2O (10:1), ultrasound; (b) BnBr, NaH, *n*-Bu_4NI, DMF; (c) IDCP, DCM/MeOH; (d) Zn, 95% EtOH, Δ; (e) Swern oxidation; (f) O_3, DCM, -78°C then Ph_3P; (g) THF, 9 M HCl; (h) 1.3 equiv of $NaCNBH_3$, MeOH; (i) 10% Pd/C, MeOH-HCOOH.

Another long synthesis of castanospermine **1a** using an olefin metathesis cyclization reaction as a key step was first revealed in 1996 then 1999 by Pandit and co-worker [260, 261]. Their method started with the gluconolactam derivative **111**, which was readily available from 2,3,4,6-tetra-*O*-benzyl-glucose by way of reductive amination of a 5-keto-gluconamide.

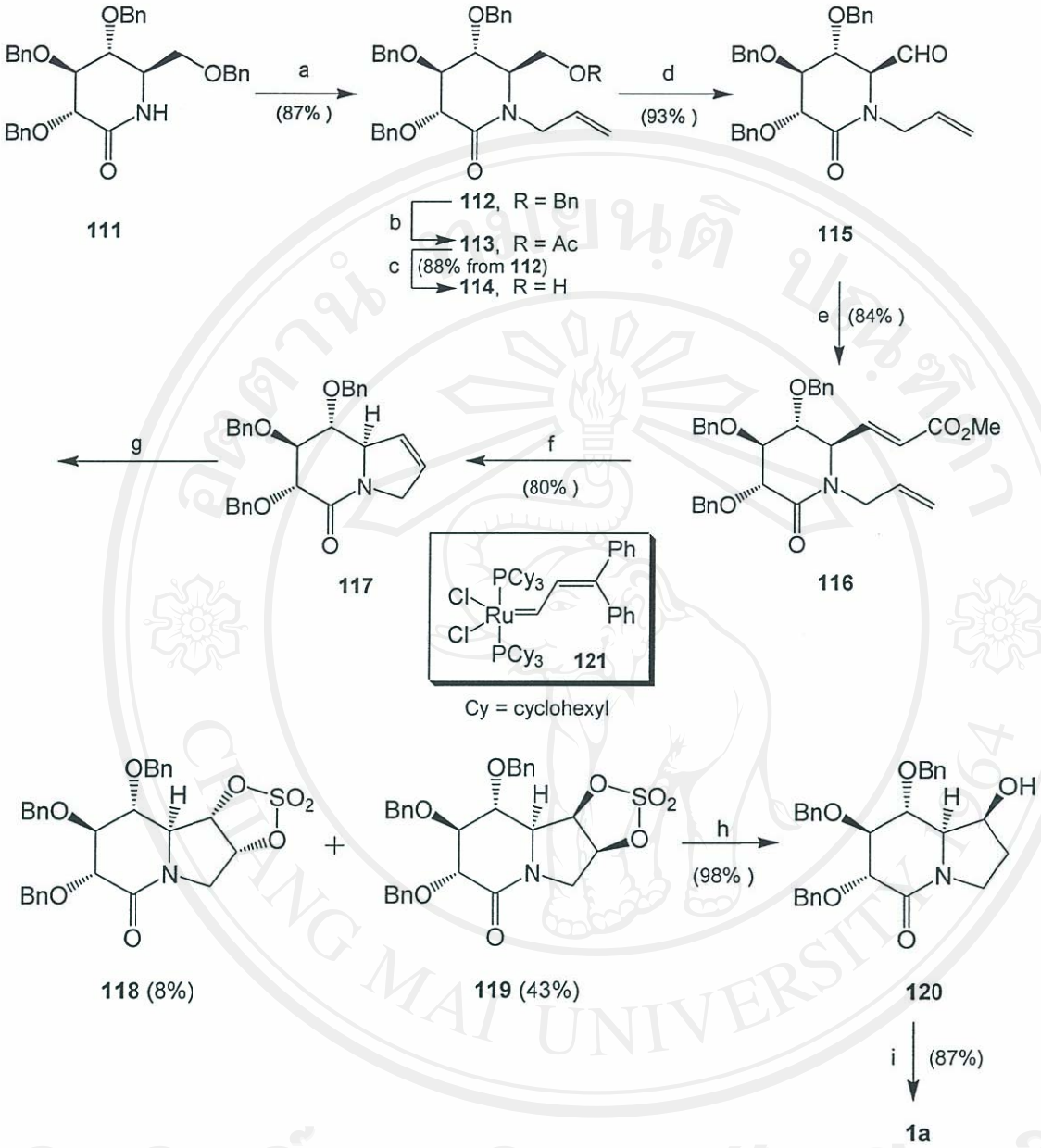

Scheme 14 *Reagents* (a) allyl bromide, KOH (50%):DCM (1:1), TBAI; (b) Ac_2O, $FeCl_3$; (c) NH_3, MeOH; (d) Dess-Martin periodinane; (e) $Ph_3P{=}CHCO_2Me$, DCM; (f) **136** (8 mol %), toluene, reflux; (g) OsO_4, NMO then $SOCl_2$, Et_3N then $NaIO_4$, $RuCl_3$; (h) BH_3, DMS; (i) H_2, Pd/C.

N-Allylation of **111** followed by selective afforded the diene **116**. This was subjected to an olefin ring-closing metathesis (RCM) reaction with the ruthenium carbene

complex **121** generating the unsaturated indolizidine **117**. Dihydroxylation of the double bond gave a mixture of *cis*-diols which were isolated as their cyclic sulfates. The major cyclic sulfate **119**, was selectively reduced and then further standard manipulations afforded castanospermine **1a**. (Scheme 14)

A divergent synthetic route to castanospermine **1a** have been developed *via* phenyl selenoamination of trichloroacetimidate **123** [262] derived from allylic alcohol **122**. The oxazoline moiety of **123** was partially hydrolyzed to give the hydroxyl trichloroacetamide then oxidative eliminated of the PhSe groups with hydrogen peroxide afforded the *trans*-olefin **124**. Pyrrolizidine **127** was derived from the desilylation of the *trans*-olefin **124** followed by Mitsunobu cyclization then *N*-protection with the Z group. Silyl ether **128** was generated from **127** by protection of the secondary hydroxy group with MOMCl, hydrolysis of the acetonide moiety and monosilylation of the primary hydroxyl group with TBDPSCl in sequence. Osmylation of **128** gave triol **129**. This was exposed to acetone in the presence of TsOH and the desired dioxolane **130** was obtained by ketalization of the two *syn*-hydroxy groups. The remaining hydroxy group of **130** was inverted by mesylation followed by desilylation to afford epoxide **131**. Removal of the Z group in **131** was anticipated to induce 6-*endo* cyclization rather than 5-*exo* cyclization due to the *anti*-arrangement of the dioxolane ring. Indeed heating **131** under catalytic transfer hydrogenation conditions provide only indolizidine **132**. Finally castanospermine **1a**, was obtained by acid hydrolysis of **132**. (Scheme 15)

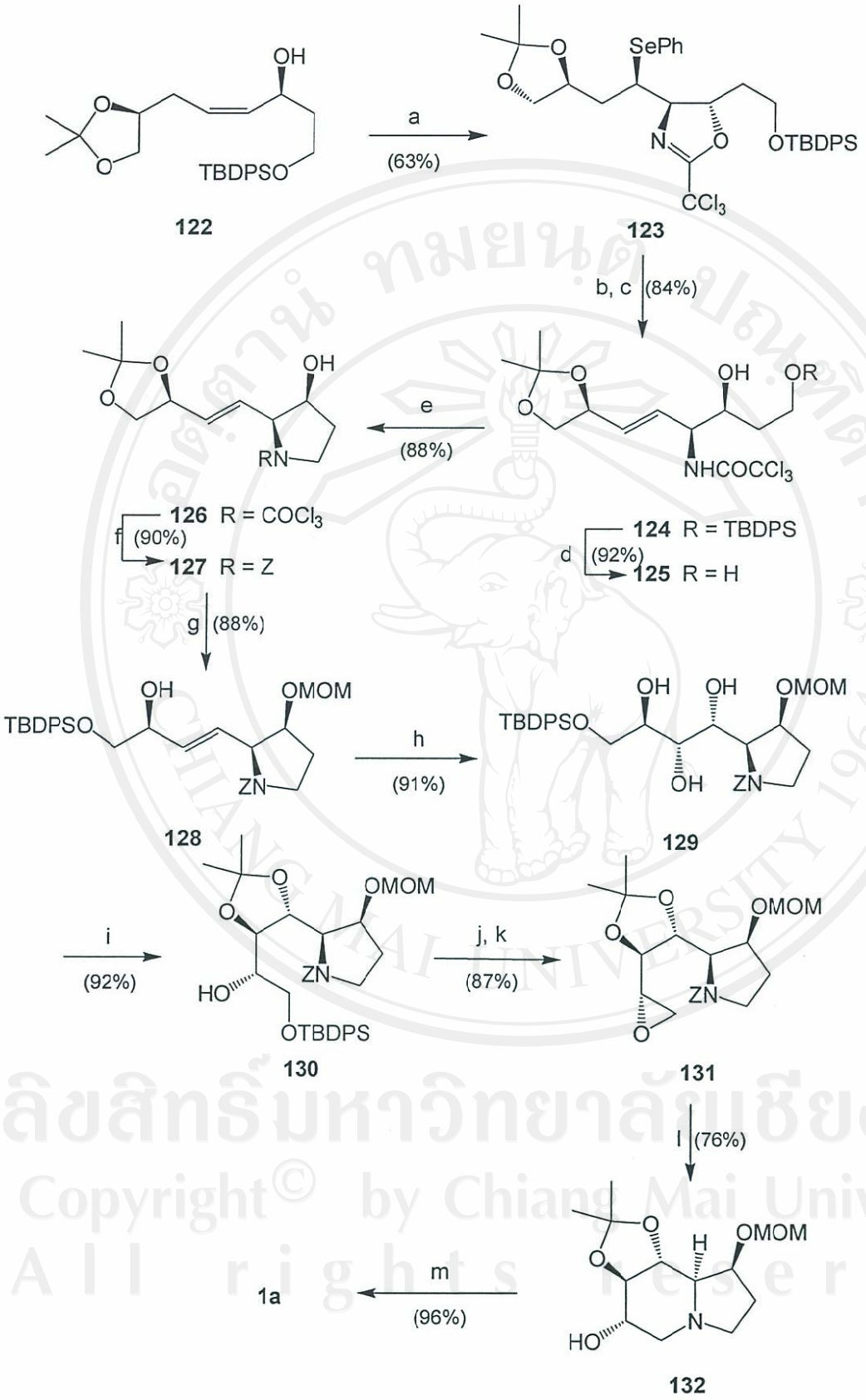

Scheme 15 *Reagents* (a) Cl_3CCN, DBU, CH_3CN, 0°C then PhSeCl, $CH_3OC(=NH)CCl_3$, Et_3N, CH_3CN, -20 to -15 °C; (b) PPTS, H_2O, MeOH, 20°C; (c) 30% H_2O_2, THF, 0-20°C ; (d)

Bu_4NF, THF, -5 to 0°C then aq. NaH_2PO_4; (e) DIAD, Ph_3P, THF, O°C; (f) NaOBn, THF, 20°C; (g) i. MOMCl, Et_3N, DCM, reflux, ii. TsOH, MeOH, 20°C, iii. TBDPSCl, imidazole, DMF, DCM, -60°C; (h) OsO_4, NMO, H_2O, acetone, 0°C; (i) TsOH, acetone, 20°C; (j) MsCl, DMAP, Et_3N, DCM, 20°C; (k) Bu_4NF, THF, 20°C then 5 M NaOH; (l) 5% Pd/C, cyclohexane, EtOH, reflux; (m) HCl (conc.) MeOH, reflux.

Denmark and Martinborough reported an efficient enatioselective synthesis of indolizidines and pyrrolizidines by using nitroso acetal **133** as the potential starting material [263]. Castanospermine **1a** is one of the desired target molecules from their route by beginning with the Sharpless asymmetric dihydroxylation of **133** to generate diol **134** as the major isomer. Selective tosylation of the primary position of diol **134** gave the tosylate **136**, which was converted to the indolizidine **131** by Ra-Ni catalytic hydrogenolysis. Deprotection of the di-*t*-butylsilyl moiety of **131** with HF in MeOH gave the fluoride salt of **1a**, and the free base was then obtained by cation exchange chromatography on AG 50W-X8 (Scheme 16).

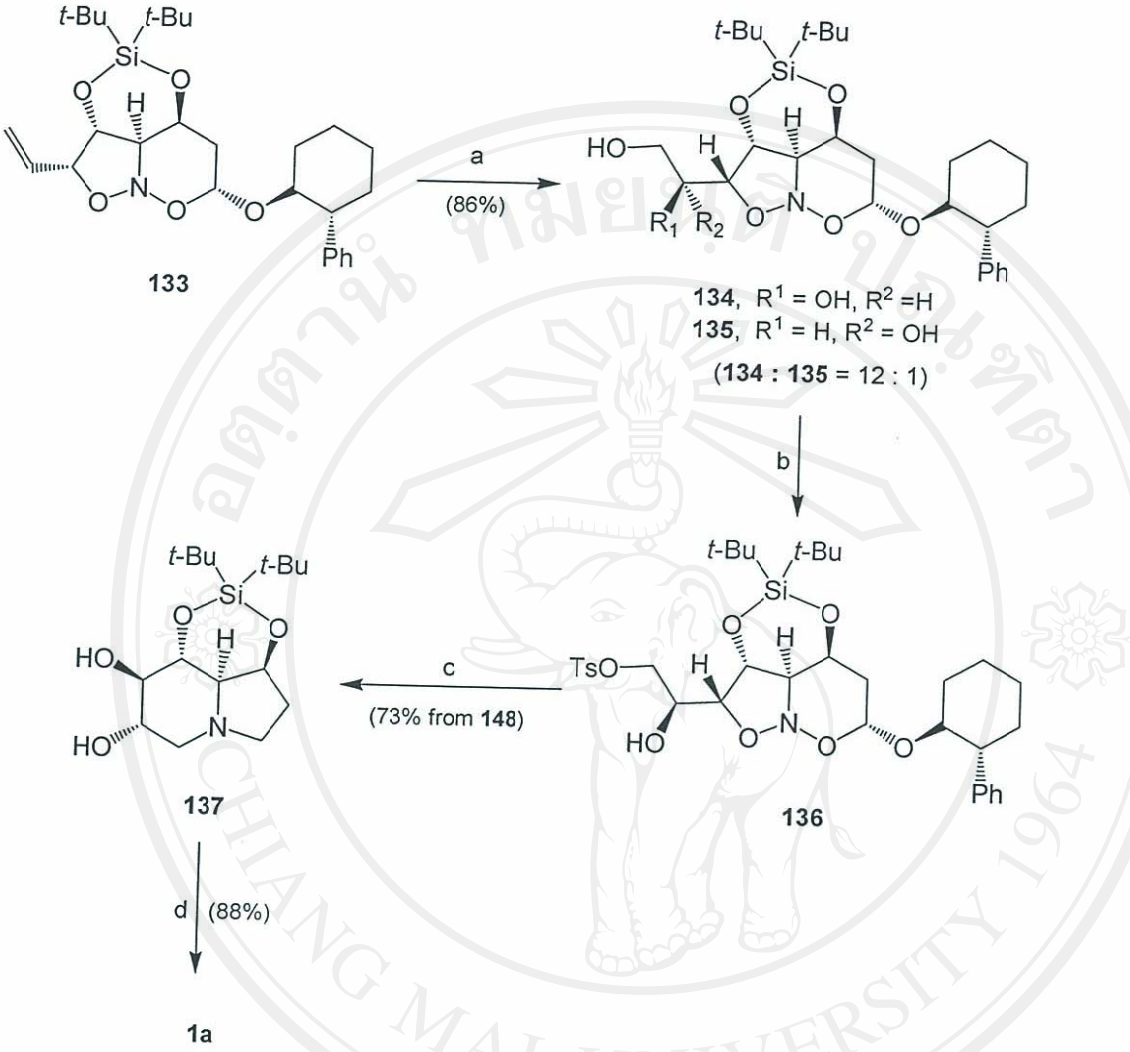

Scheme 16 *Reagents* (a) $K_2OsO_2(OH)_4$, K_2CO_3, H_2O, $NaHCO_3$, $K_3Fe(CN)_6$, *t*-BuOH, $(DHQD)_2$-AQN; (b) TsCl, Pyridine, rt, 3.5 h; (c) H_2, Ra-Ni, 160 psi, MeOH, 36 h; (d) HF, MeOH, rt, 24 h, then AG 50W-X8.

In 2003, Somfai and co-worker reported the synthesis of castanospermine **1a** [264] (Scheme 17). Their reaction started with a regioselective Sharpless asymmetric dihydroxylation of diene **138**, the resulting diol was protected as an acetonide, prior to reduction of the ester with DIBAL to give the allylic alcohol **140**. Sharpless asymmetric epoxidation gave the oxirane alcohol, which was protected as a TBDPS

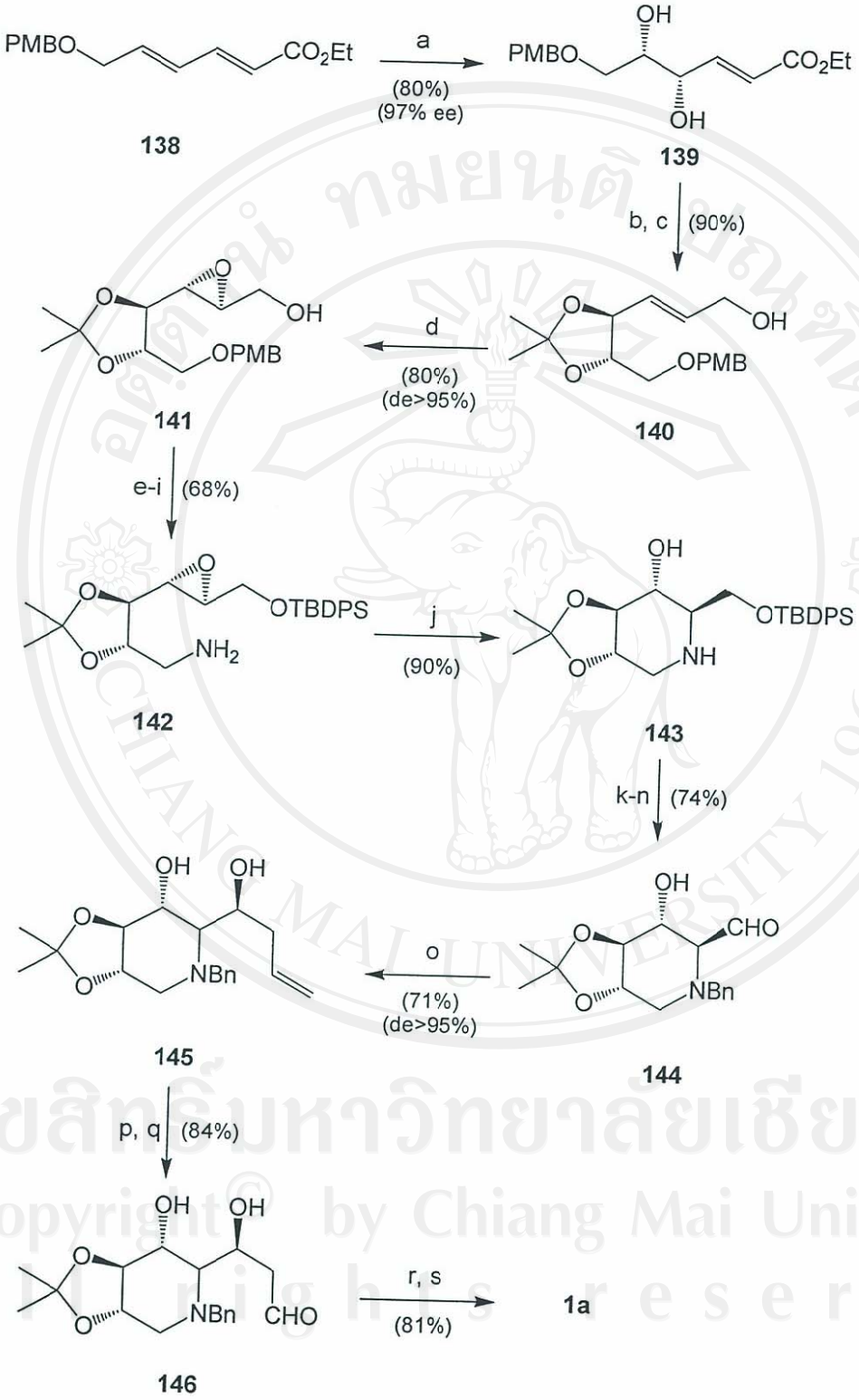

Scheme 17 *Reagents* (a) AD-mix-α, $K_2OsO_4.2H_2O$, $MeSO_2NH_2$, *t*-BuOH/H_2O (1:1), 0°C; (b) H_2C=C(OMe)Me, *p*-TsOH (cat.), DMF, rt; (c) DIBAL, DCM, -78°C, then MeOH; (d) (+)-diisopropyl tartate, $Ti(O^iPr)_4$, *t*-BuOOH, DCM, -20°C; (e) TBDPSCl, Et_3N, DMAP (5

mol%), DCM, rt; (f) DDQ, DCM, H_2O, 0°C to rt; (g) $MeSO_2Cl$, *i*-Pr_2NEt, DCM, rt; (h) NaN_3, DMF, 80°C; (i) PPh_3, THF/H_2O (10:1), rt; (j) EtOH, reflux, 65 h; (k) BnBr (3 equiv), KHMDS (2.2 equiv), THF, -78°C to rt; (l) BnBr (1.3 equiv), K_2CO_3 (2.6 equiv), MeCN, reflux; (m) $Bu_4NF{\cdot}2H_2O$, THF, rt; (n) DMSO, $(COCl)_2$, Et_3N, DCM, -78°C to rt; (o) $H_2C{=}CHCH_2SiMe_3$, $TiCl_4$, DCM, -65°C, 15 h; (p) NMO, OsO_4 (cat.), *t*-BuOH/THF/H_2O (10:3:1), rt; (q) $NaIO_4$, $NaHCO_3$, THF/H_2O (1:1), rt; (r) H_2, 10% Pd/C, EtOAc, rt; (s) TFA/H_2O (8:1), rt, then chromatography on Dowex 1-X, OH^- form.

ether. The PMB group was then removed oxidatively using DDQ, and the resulting alcohol was converted to the azide via the corresponding mesylate. Staudinger reduction of the azide gave amine **142**, which underwent cyclization to piperidine **143**. This was *N*-benzylated in two steps, then TBDPS removal and Swern oxidation gave aldehyde **144**. Sakurai allylation of **144** was followed by dihydroxylation of the new allyl double bond and oxidative cleavage of the diol gave the homologated aldehyde **146**. Finally, reductive amination with an acidic workup produced castanospermine **1a**.

Mariano and co-worker [265] reported the ring rearrangement metathesis (RRM) reaction of the enatiomerically enriched *cis*, *trans*-*N*-allylacetamidocyclopentendiol derivative **147**, proceed smoothly to furnish the corresponding 6-allyltetrahydropyridine **149**. This highly regioselective precess was performed using the second generation Grubbs ruthenium akylidine catalyst **148** in the presence of ethylene. Allylic alcohol **150** was derived by treatment of **149** with TBAF, followed by *N*-acetylation of the resulting product [266]. The selective epoxidation of **150** produced the corresponding epoxy-alcohol **151**. *trans*-Diaxial ring opening of **151** under mild basic conditions furnished the trihydroxy piperidine **152**. Benzylation of

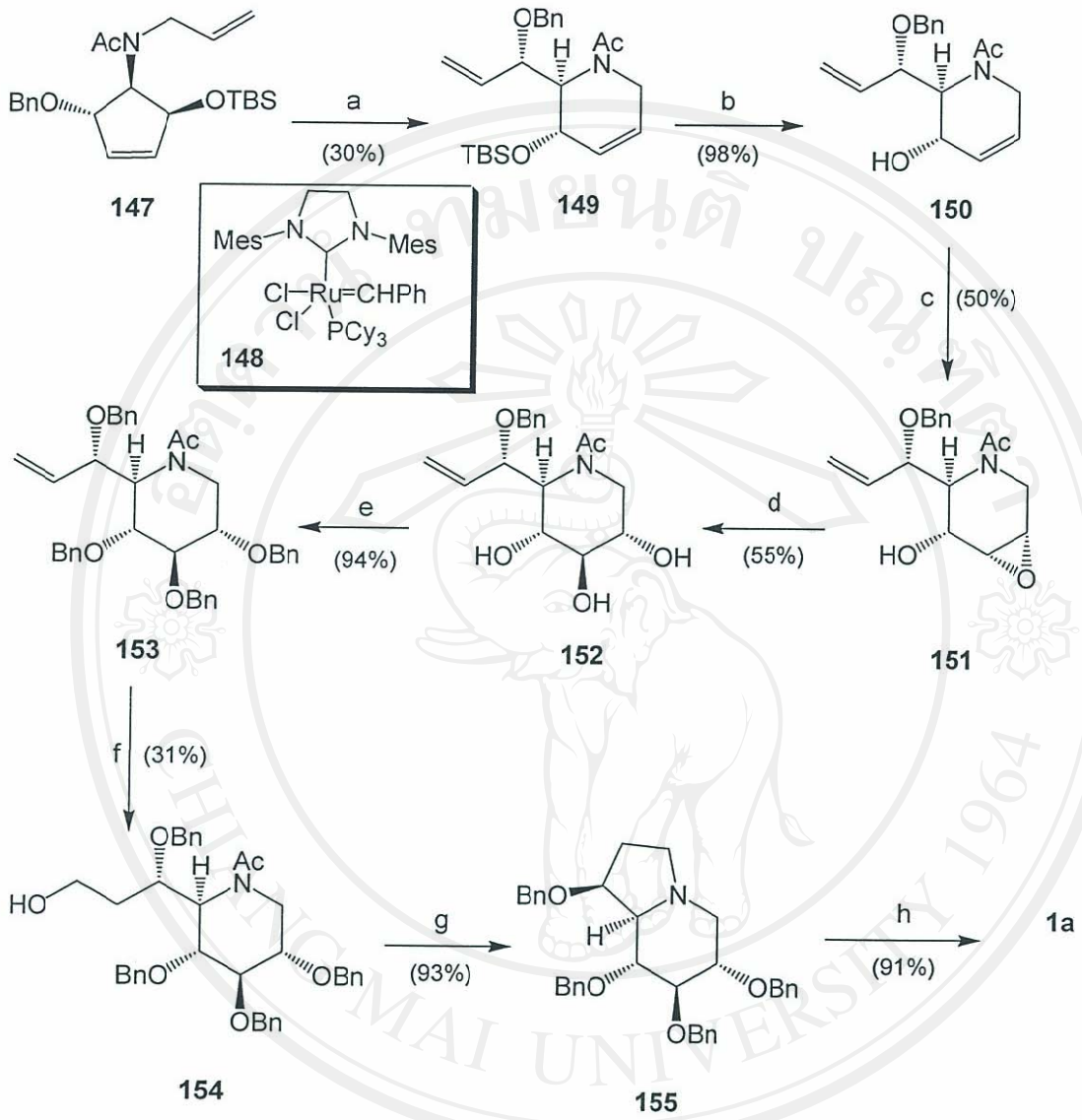

Scheme 18 *Reagents* (a) **148**, ethylene, DCM, reflux, 16 h; (b) TBAF, THF, rt, 2 h; (c) $VO(acac)_2$, *t*-BuOOH, DCM, rt, 5 h; (d) NaOBz (aq.), 130°C, 12 h; (e) NaH, BnBr, DMF, 0°C, 2 h; (f) BH_3-THF, 0°C, 3 h, then 3 M NaOH, H_2O_2, rt, 3 h; (g) DEAD, Ph_3P, THF, rt, 12 h; (h) H_2, Pd/C, MeOH, rt, 4 h.

152 provided the tetrabenzyl ether **153**. After treatment of the result with the BH_3-THF complex followed by NaOH-H_2O_2 oxidation afforded the alcohol **154**. Indolizidine ring formation took place when **154** was subjected to typical Mitsunobu

cyclization conditions to yield indolizidine **155**. Hydrogenolytic removal of the benzyl protecting groups then generated the target castanospermine **1a** (Scheme 18).

Murphy and co-worker presented a novel synthesis of castanospermine **1a** from the 6-deoxyhex-5-enopyranoside, **156** [267]. The acetate groups of **156** were removed, and benzyl protecting groups were introduced to give **157**. Oxidation using methyl(trifluoromethyl)dioxirane generated *in situ* gave a 1.7:1 mixture of epoxides **158**. Treatment of the epoxides with methanol in the presence of camphosulfonic acid gave a mixture of 5-*C*-methoxy-D-glucopyranosyl azide **159** and 5-*C*-methoxy-L-idopyranosyl azide **160**. This mixture was oxidized to the separable aldehyde **161** and **162** by treatment with tetra-*n*-propylammonium perruthenate and NMO. The aldol reaction of **162** with LDA and EtOAc gave a mixture of diastereoisomeric alcohols **163** and **164**. The separated **164** was further reduced to form the cyclic lactam **17**. Reduction of **17** was achieved by protection of hydroxyl groups as TMS ethers and subsequent reaction using $LiAlH_4$, giving castanospermine **1a**. The same procedure applied to **163** gave (+)-1-epicastanospermine **1c**. (Scheme 19)

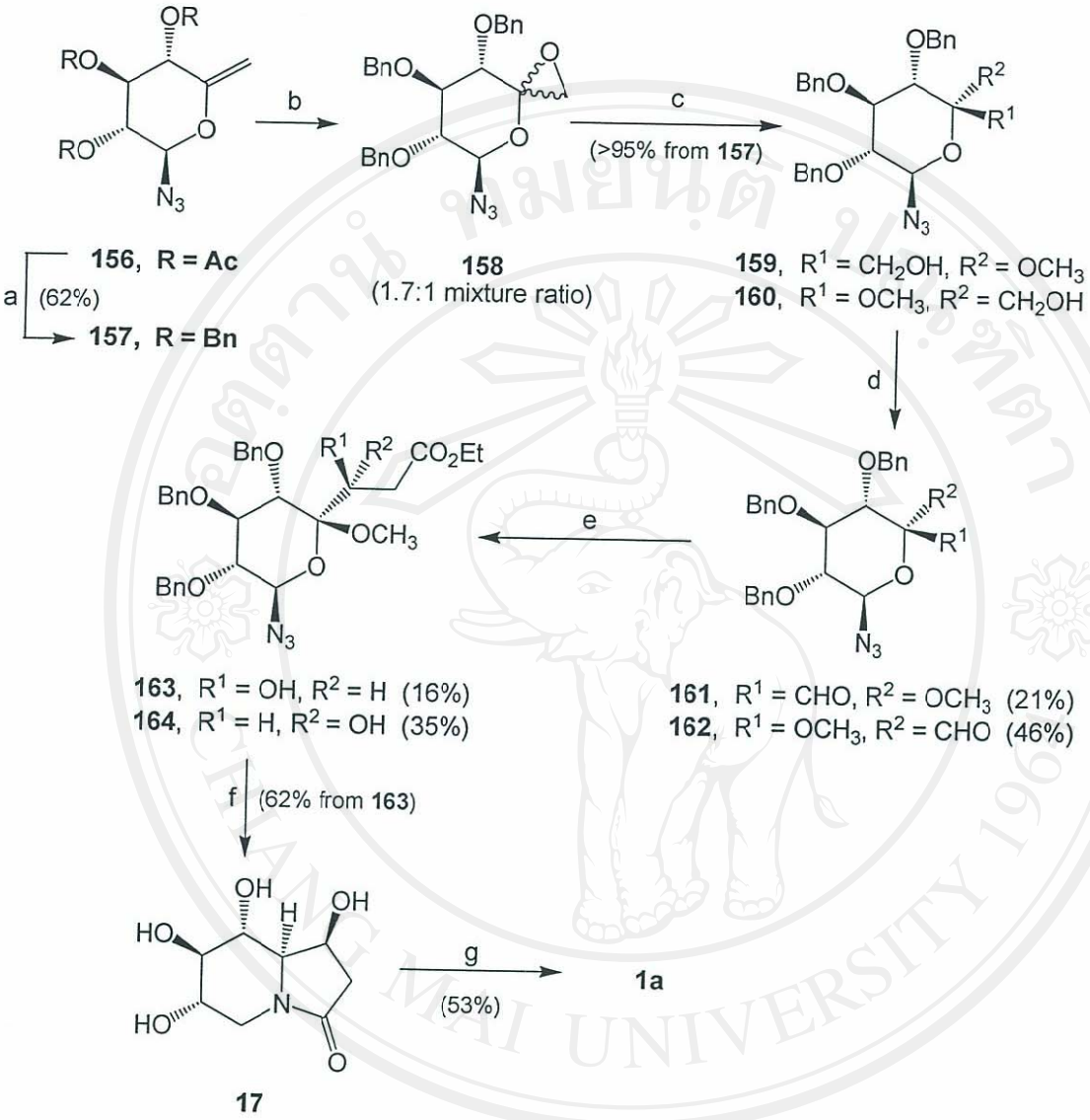

Scheme 19 *Reagents* (a) i. NaOMe, MeOH, rt, 1 h, ii. BnBr, DMF, 0°C, 3 h; (b) 1,1,1-trifluoroacatone, oxone, $NaHCO_3$, NaEDTA, CH_3CN, H_2O, 0°C, 1.5 h; (c) CSA, MeOH, 10 min; (d) TPAP, NMO, DCM, 4 Å molecular sieves, rt, 15 h; (e) LDA, EtOAc, THF, -78°C to rt, 1.5 h; (f) $Pd(OH)_2$, H_2, MeOH, HCO_2H, 500 psi, rt, 48 h.; (g) i. TMSOTf, pyridine, 2,6-lutidine, 0°C to rt, 12 h, ii. $LiAlH_4$, THF, 16 h.

More recently (2006) the total synthesis of castanospermine **1a** was revealed by Dhavale and co-worker [268]. Their synthesis involved a intramolecular 5-*endo*-trig aminomercuration of *β*-hydroxy-*γ*-alkenylamines **171** as an efficient key step to

generate the pyrrolidine ring which could be applied to castanospermine **1a** and its epimers. A 1,3-addition reaction of vinylmagnesium bromide to nitrone **165** afforded a mixture of **166a** and **166b** in a ratio of 79:11. Then N-O bond reductive cleavage in **166a** generated the *N*-benzylamino sugar **167**. Treatment of **167** with benzylchloroformate afforded the *N*-Cbz protected derivatives **168**. The α-amino aldehyde **169** was derived from the dihydroxylation of **168** followed by oxidative cleavage of the resulting diol. In the next step, the reaction of vinylmagnesium bromide with α-amino aldehyde **169** at -50°C afforded an inseparable diastereomeric mixture of **170a** and **170b**. The mixture was treated with 40% KOH in methanol at 90°C for 10 min to give the separable carbamates **171a** and **171b** in a ratio of 3:1. The reaction of **171a** with mercury (II) acetate in THF-water at room temperature, followed by the reductive demercuration with $NaBH_4$ and benzylation afforded dibenzylate pyrrolidine **172**. The pyrrolidine derivative **172** was found to be the precursor for the synthesis of the target molecule, castanospermine **1a**. Thus, hydrogenolysis of the *N*- and *O*-benzyl groups in **172**, followed by selective amine protection, afforded the *N*-Cbz protected compound **173**. Finally, deprotection of the acetonide moiety using TFA-water followed by hydrogenolysis afforded castanospermine **1a** (Scheme 20).

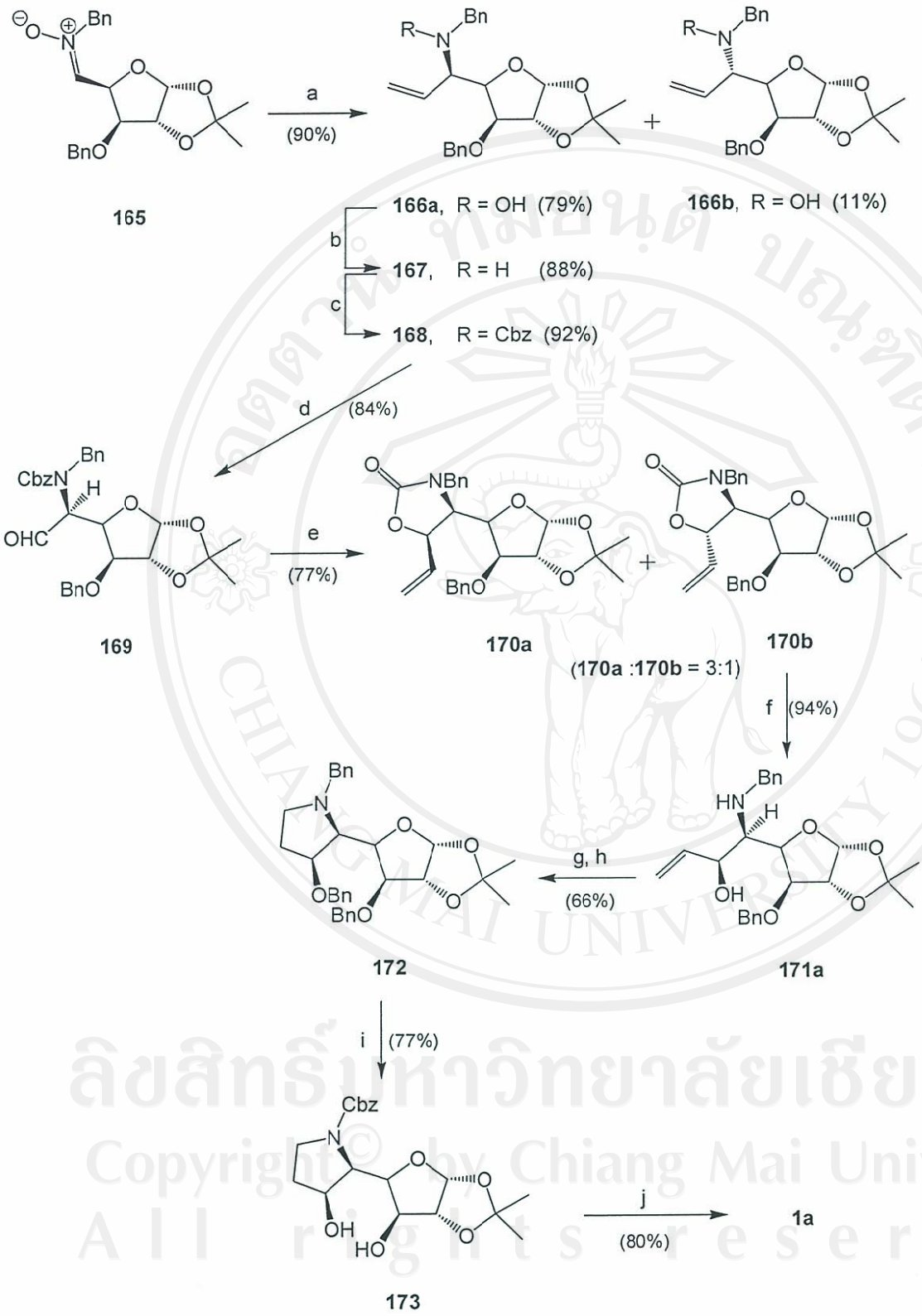

Scheme 20 *Reagents* (a) vinylmagnesium bromide, TMSOTf, THF, -78°C, 2 h; (b) Zn, $Cu(OAc)_2$, AcOH, 80°C, 1 h; (c) $NaHCO_3$, CBzCl, MeOH-water (4:1), 3 h; (d) i. NMO, $K_2OsO_4 \cdot 2H_2O$, acetone-water (8:1), 12 h, ii. $NaIO_4$, acetone-water (9:1), 6 h; (e) i.

vinylmagnesium bromide, THF, -50°C, 1 h, ii. 40% KOH, MeOH, 90°C, 10 min; (f) 40% KOH, MeOH, 90°C, 48 h; (g) $Hg(OAc)_2$, THF-water (1:1), $NaBH_4$, 3 h; (h) NaH, BnBr, TBAI, THF, 0°C to rt, 6 h; (i) i. $HCOONH_4$, 10%Pd/C, MeOH, 80°C, 1 h, ii. $NaHCO_3$, CbzCl, MeOH-water (9:1), 3 h; (j) i. TFA-water (3:2), 2.5 h, ii 10% Pd/C, MeOH, 80 psi, 12 h.

1.4 Aims of This Project and Proposed Synthetic Approach

In this project, we aim to develop a new synthetic strategy for the preparation of (+)-castanospermine **1a** as shown in Scheme 21.

This approach, suggested that the target compound could be acquired from the precursor **176** using a ring-closing matathesis (RCM) reaction with the Grubbs catalyst, osmium (VIII) *syn*-dihydroxylation, and Mitsunobu cyclization to form the indolizidine ring. The 1,2-*anti* amino alcohol **176** would be expected to be readily obtained from the boronic-Mannich reaction (Petasis reaction) of L-xylose, allylamine, and (*E*)-styrene boronic acid, followed by chemo- and regioselective *N*- and *O*-protection reactions. The successful of this synthetic scheme is discussed in the following chapter.

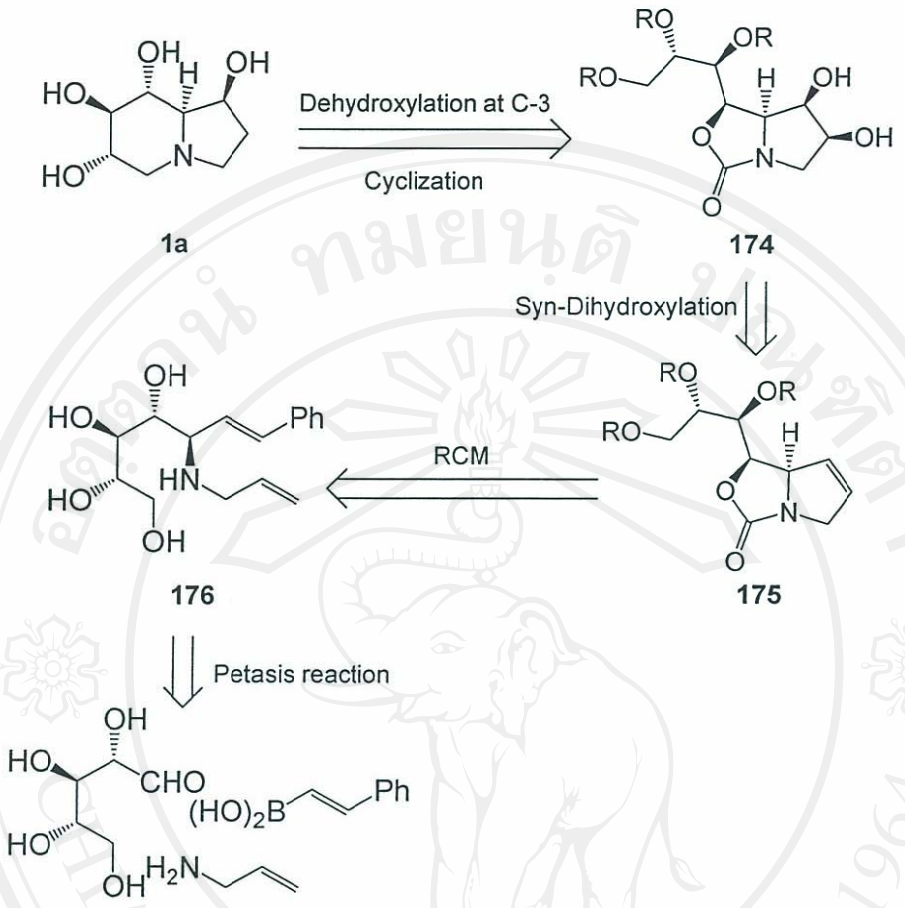

Scheme 21 Retrosynthetic analysis of (+)-castanospermine (**1a**)